

Status and Prospect of MJ Plasma Focus Experiment

by

Marek Scholz

Institute of Plasma Physics and Laser Microfusion

Warsaw, Poland



Outline

1. Introduction

- Goals of experiment

2. Time evolution of PF discharge for two kinds of electrodes correlated with neutron emission

- Visualization of the pinch dynamics and structure

3. Neutrons measurements

4. Summary



Neutron yield Y_n

$$P = \frac{N_D n_D}{4} \cdot \langle \sigma \mathbf{v} \rangle \cdot \tau$$

$$n_D = \frac{N_D}{\pi a^2}$$

$$N_D = \frac{I^2}{4c^2 T}$$

$$\tau = \alpha \frac{a}{v}$$



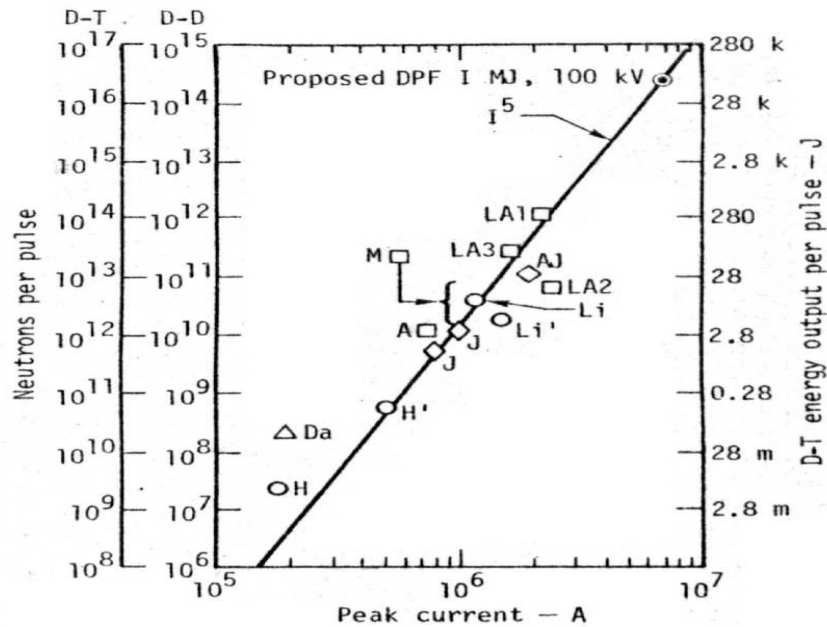
$$Y_n = l \cdot P \propto \alpha \frac{l}{a} I^4 \frac{\langle \sigma \mathbf{v} \rangle}{T^{5/2}}$$

for $T = 9 \text{ keV}$

$$Y_n = 1,6 \cdot 10^7 \alpha \frac{l}{a} I^4$$



Scaling



Legend

- AJ Aerojet Nucleonics. 250 kJ, 20 kV, 320 μ F.
- Da Darmstadt. 0.34 - 1.35 kJ; 10 - 20 kV.
- H Hoboken. Electrode structure is identical to that of Darmstadt group.
- H' Hoboken. About 5 kJ.
- A^E Aerospace Corporation.
- J Julich. 25 kJ; 40 kV.
- Li Limeil. 96 kJ, 40 kV.
- Li' Limeil. Plasma focus driven by explosive generator.
- LA¹ Los Alamos. DPF-6; 420 kJ.
- LA² Los Alamos. DPF-5; 120 kJ.
- LA³ Los Alamos. DPF-6; 210 kJ.
- M Moscow. $\gamma \rightarrow 10^{10}$ to 10^{11} DD neutrons; I = 1 MA.



Large PF device

PF – 3 (Moscow), $E_b = 3 \text{ MJ}$, $U_b = 20 \text{ kV}$;

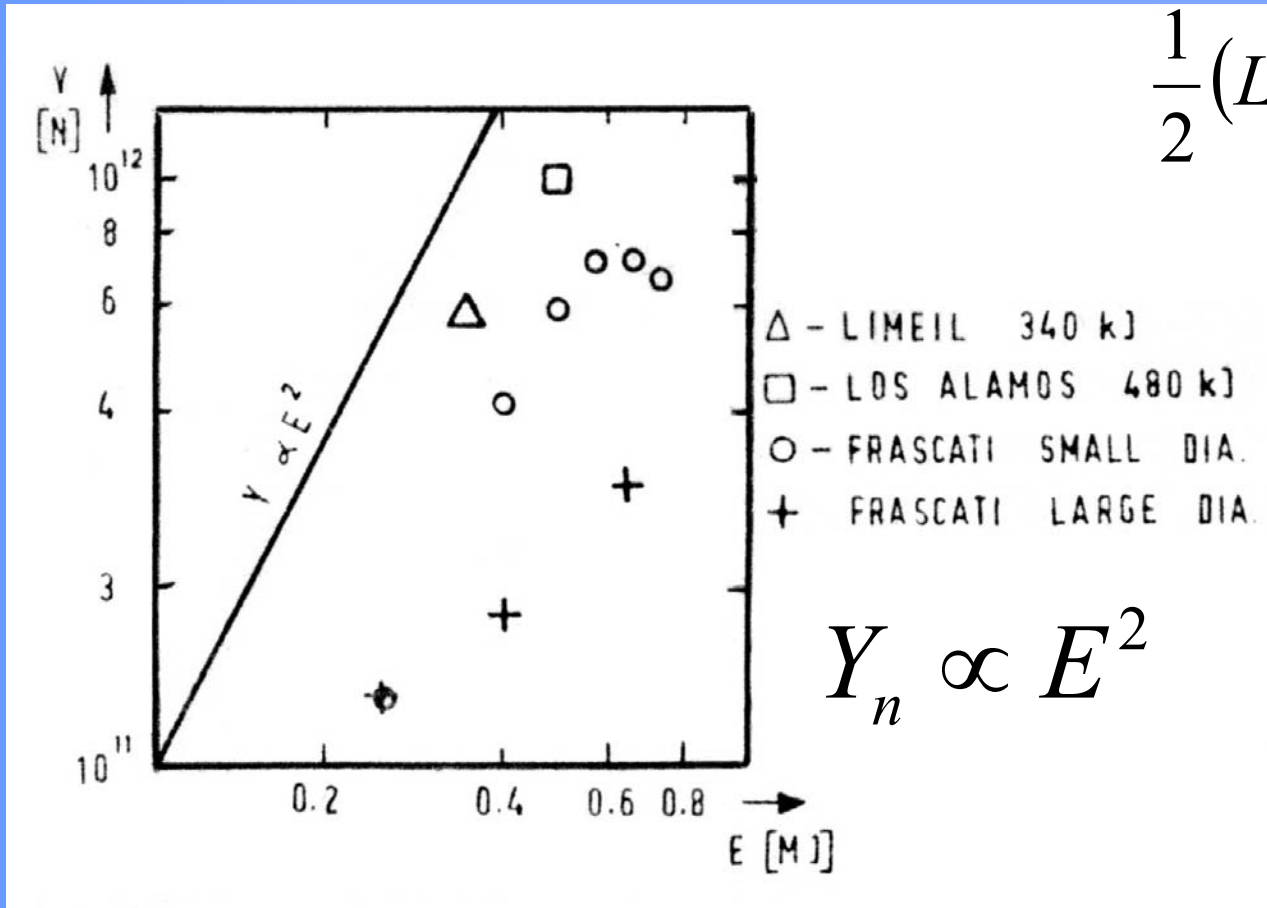
Frascati (Program Euroatom), $E_b = 1 \text{ MJ}$; $U_b = 50 \text{ kV}$;

Poseidon (Stuttgart), $E_b = 750 \text{ kJ}$; $U_b = 80 \text{ kV}$;

PF-1000 (Warsaw), $E_b = 1 \text{ MJ}$; $U_b = 40 \text{ kV}$



Scaling



$$\frac{1}{2}(L + L_0)I^2 \cong \gamma E$$

$$L \cong L_0$$

$$Y_n \propto E^2$$

$$I^2 \propto E$$

Frascati (Program Euroatom), $E_b = 1\text{MJ}$; $U_b = 50\text{ kV}$;



Main Questions

This observed saturation in the Y_n is caused by the incorrect formation of a proper plasma sheath due to many reasons (e.g. impurities, sheath instabilities)

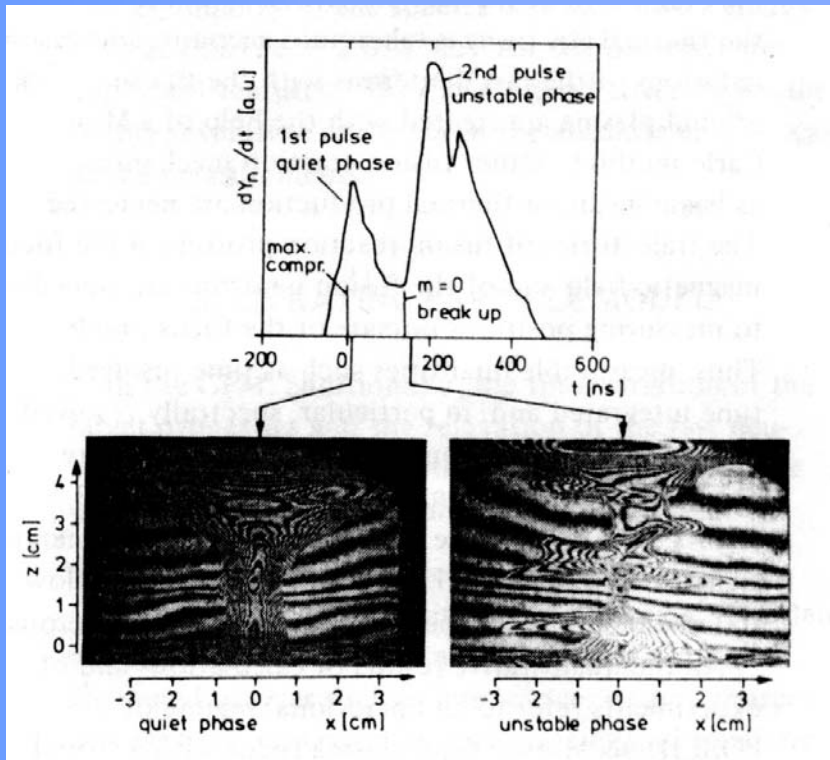
or

There exists a fundamental threshold for saturation in the Y_n

Mechanism of neutron production in
large PF facilities



Poseidon (Stuttgart)



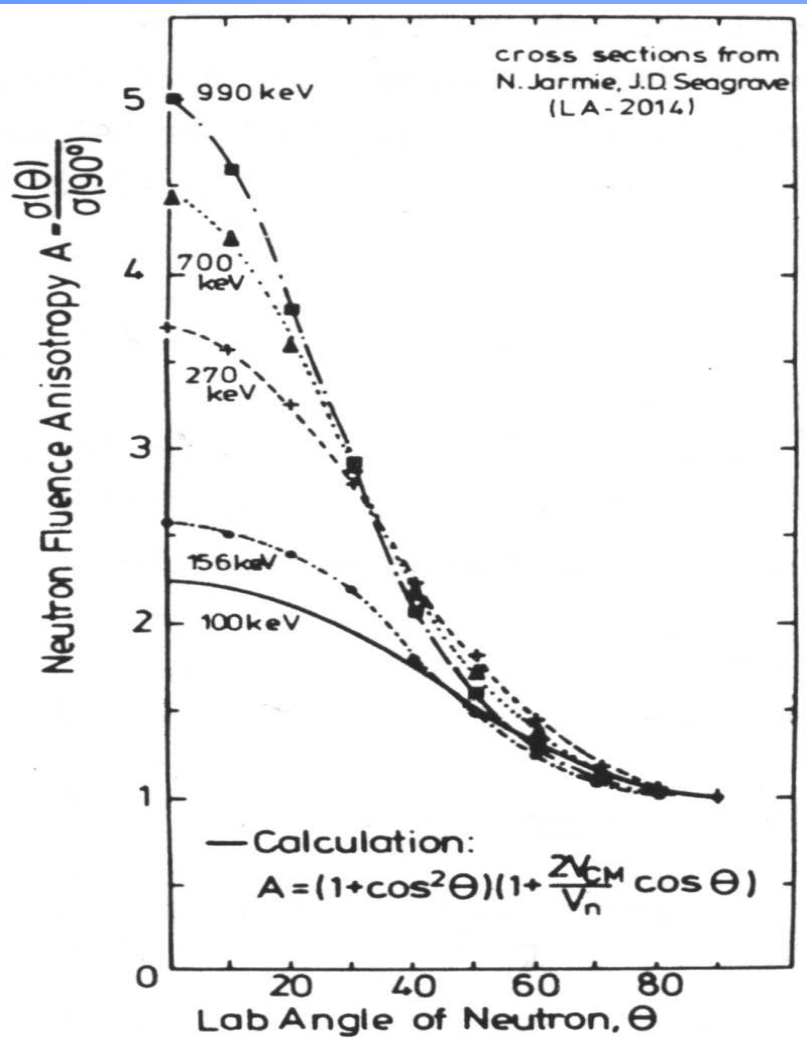
Typical neutron signal on Poseidon

- the compression phase ($t < 0$)
- the quiescent phase (plasma expands to $r \approx 2r_{\min}$)
- the instability phase ($m=0$)
- break-up of the plasma column caused by instability

Beam-Target !?



Anisotropy



$$A = \frac{Y(0^\circ)}{Y(90^\circ)} > 1$$

$$E_n(0^\circ) = \frac{3}{4} \left(Q + \frac{E_d}{2} \right) \left(1 + \frac{v}{u} \right)^2 ;$$

| | | | |
|-------------------------|------|------|------|
| $E_D(\text{keV})$ | 20 | 100 | 300 |
| $E_n(0^\circ)$ (MeV) | 2.56 | 2.80 | 3.06 |



Goals of Experiment

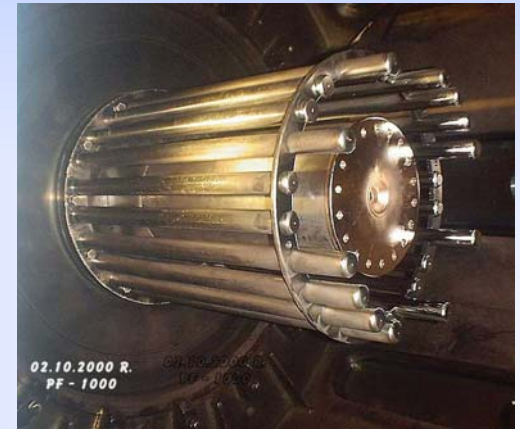
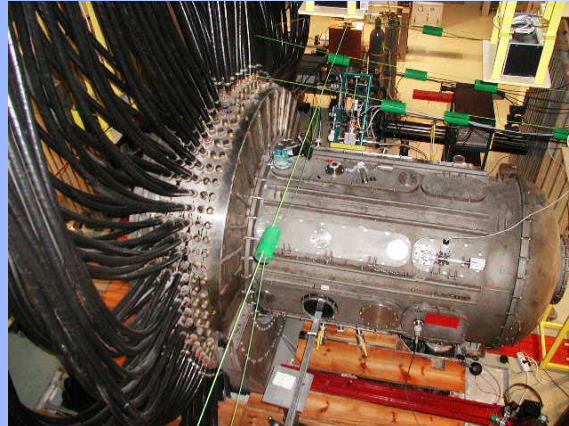
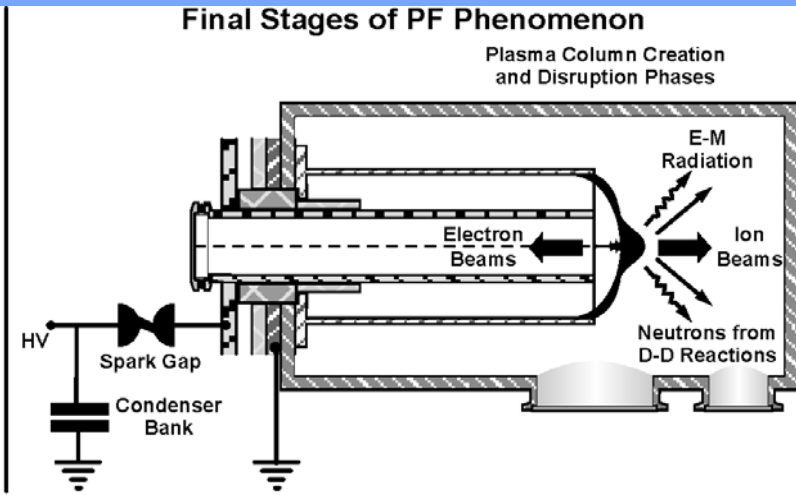
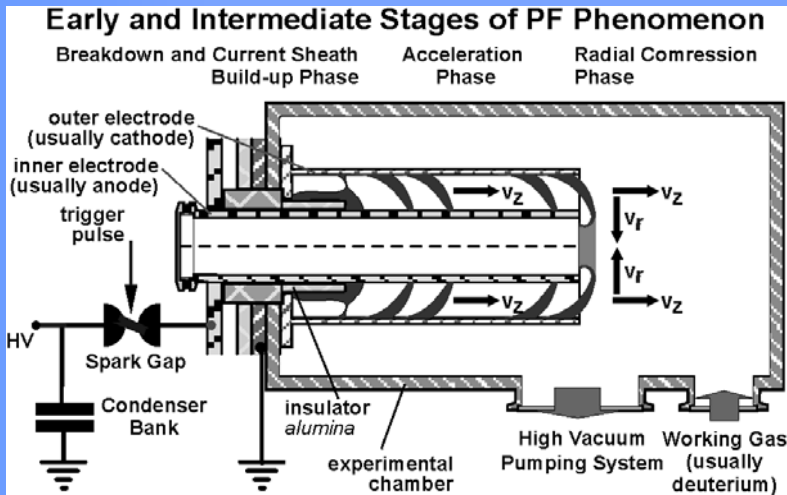
Definition of the neutron emission characteristics (**neutron anisotropy and spectra**) from large PF facility;

Definition of the relation between the Y_n and plasma sheath dynamics, with particular attention paid to structures appearing within the pinch column;

Definition of correlation between the neutron generation and other types of ionizing radiation produced within PF discharges, i.e. fast electrons, protons from DD reaction, soft and hard X-rays, etc



Apparatus



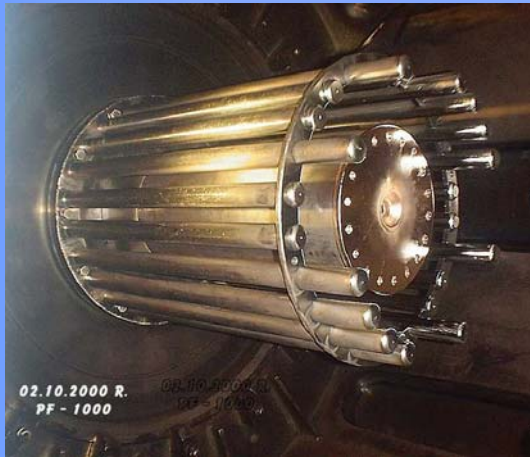
Generator PF-1000



the charging voltage - $U_0 = 20 - 40 \text{ kV}$,
the bank capacitance - $C_0 = 1.332 \text{ mF}$,
the bank energy - $E_0 = 266 - 1064 \text{ kJ}$,
the nominal inductance - $L_0 = 15 \text{ nH}$,
the quarter discharge time - $T_{1/4} = 6 \text{ } \mu\text{s}$,
the short-circuit current - $I_{SC} = 12 \text{ MA}$,
the characteristic resistance - $R_0 = 2.6 \text{ m}\Omega$,



Electrodes



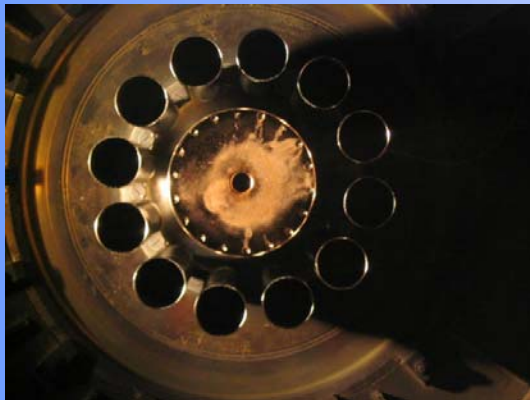
CE diameter - 226 mm

OE diameter - 400 mm

OE consists 24 rods (diam. 32 mm)

length of electrode - 560 mm

length of insulator - 113 mm



CE diameter - 226 mm

OE diameter - 400 mm

OE consists 12 rods (diam. 80 mm)

length of electrode - 560 mm

length of insulator - 113 mm



Diagnositics

$$P = \frac{N_D n_D}{2} \cdot \langle \sigma v \rangle \tau \quad Y_n = l \cdot P \propto \alpha \frac{l}{a} I^4 \cdot \frac{\langle \sigma v \rangle}{T^{5/2}}$$

Frame cameras;
Streak camera

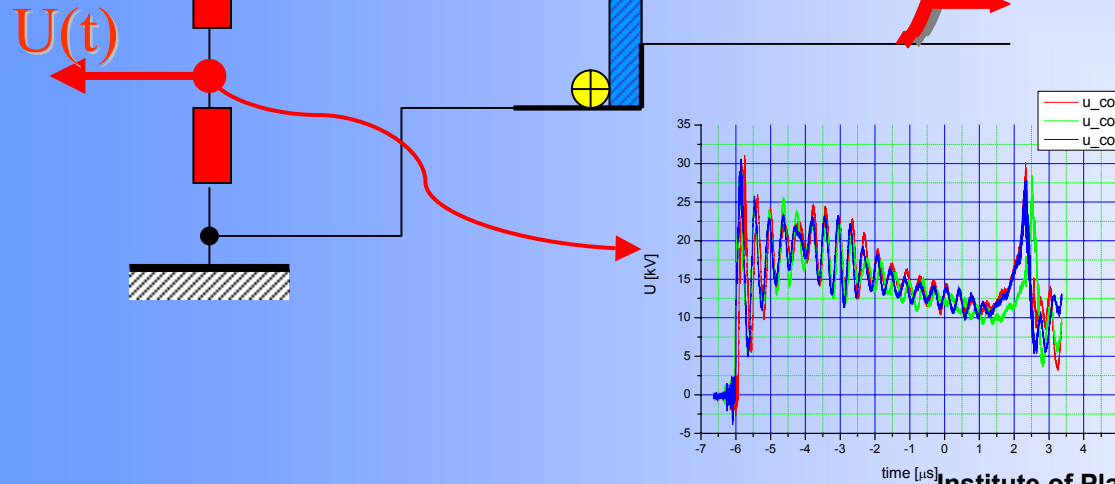
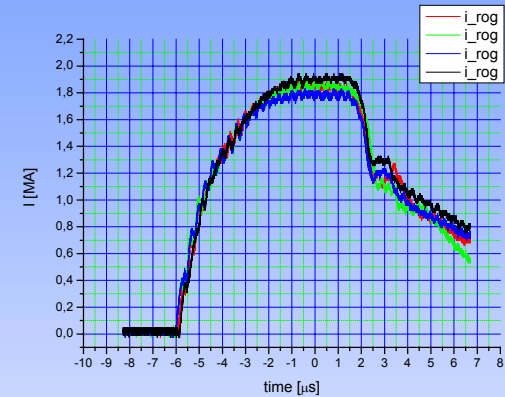
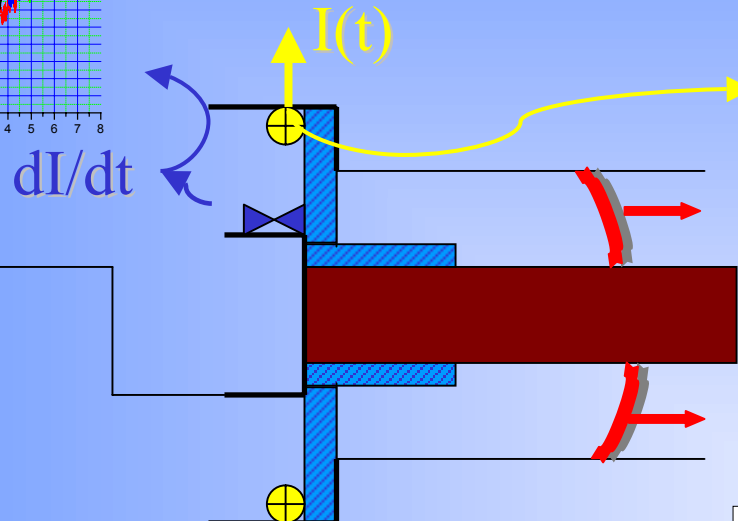
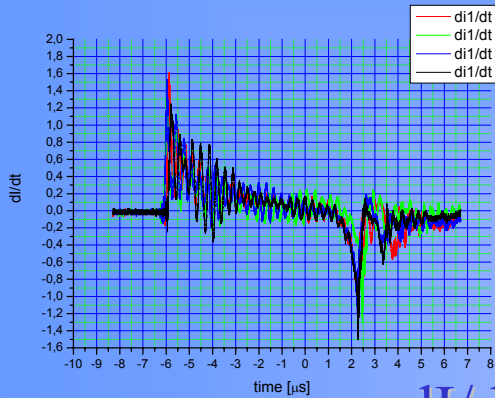
Silver Activation Counter
(anizotropy)
PMT
TOF (spectra → T)

Rogovski coil





Measurements of Current and Voltage



$$U_b = 27 \text{ kV}, E_b = 480 \text{ kJ},$$

$$p = 3,5 \text{ Torr}$$

$$Y = 5 \cdot 10^{10} - 3 \cdot 10^{11}$$



Compression, Pinch & Post-pinch



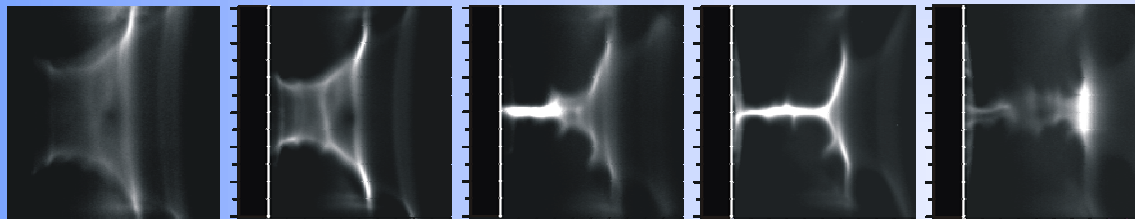
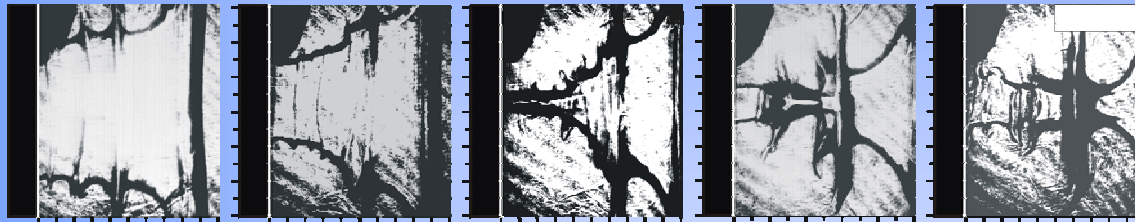
-170 ns

-120 ns

0 ns

50 ns

140 ns

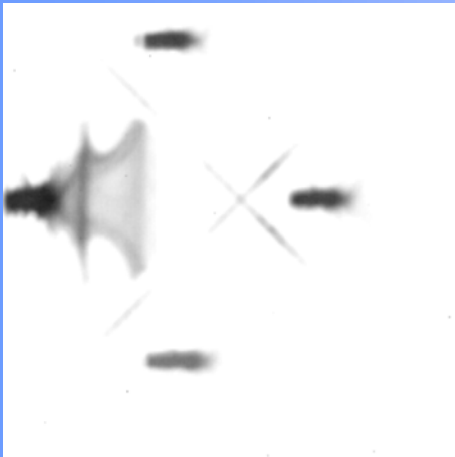


Visible frames - exposure time 1 ns, window 589 nm





Compression, Pinch & Post-pinch

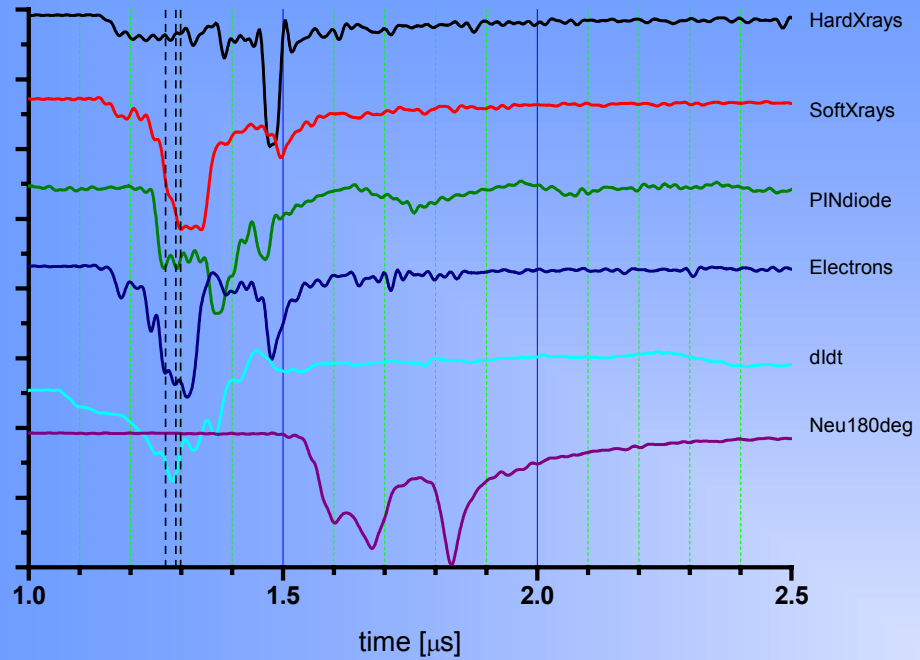


XUV frames - exposure time 2 ns, window 200-300 eV+above 600 eV

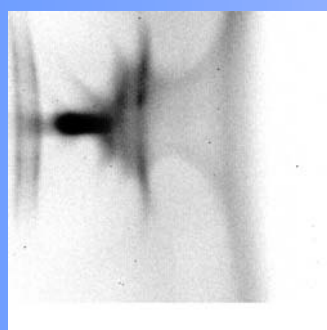




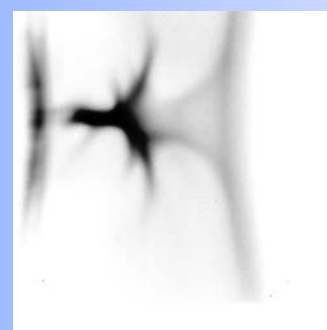
shot 3108



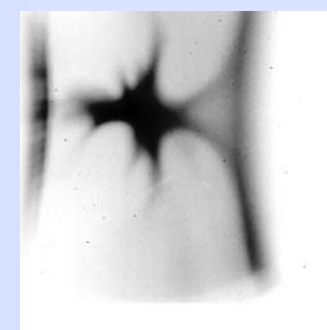
$p = 3.00$ Torr
 $U_b = 33.0$ kV
 $E_b = 734.0$ kJ
 $I_{max} = 1.66$ MA
 $L_1 = 77897$
 $L_2 = 66392$
 $L_3 = 47298$
 $L_4 = 78015$
 $L_5 = 31732$



1.269 μ s



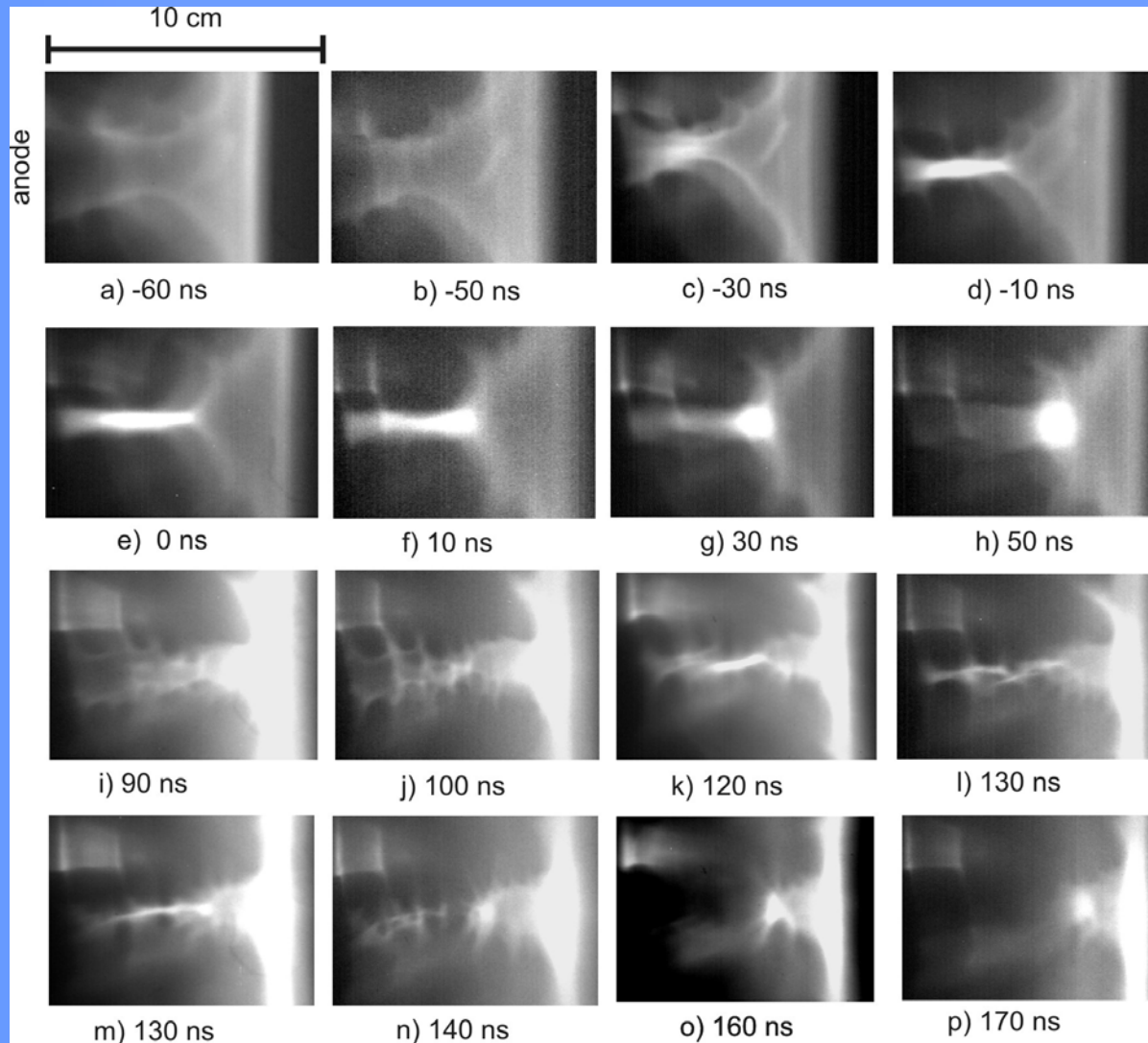
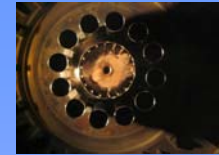
1.289 μ s



1.299 μ s



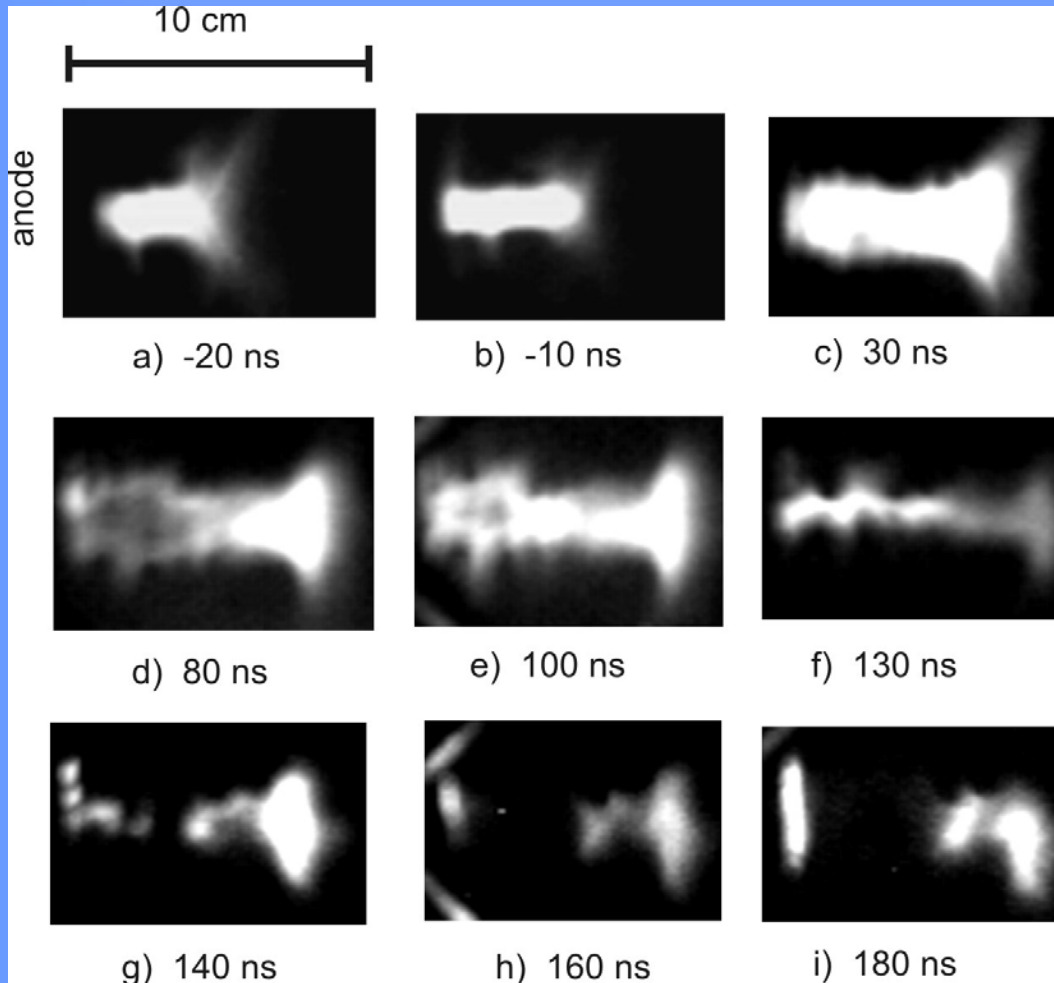
Visible frames - exposure time 1 ns, window 589 nm



a-d *implosion 2×10^5 m/s*
e *minimum radius $t=0$*
c-g *intense light - dense plasma, dense spherical structure*
g-p *instabilities*
j-m *second pinch*
m-n *second explosion*
m-p *second dense structure*



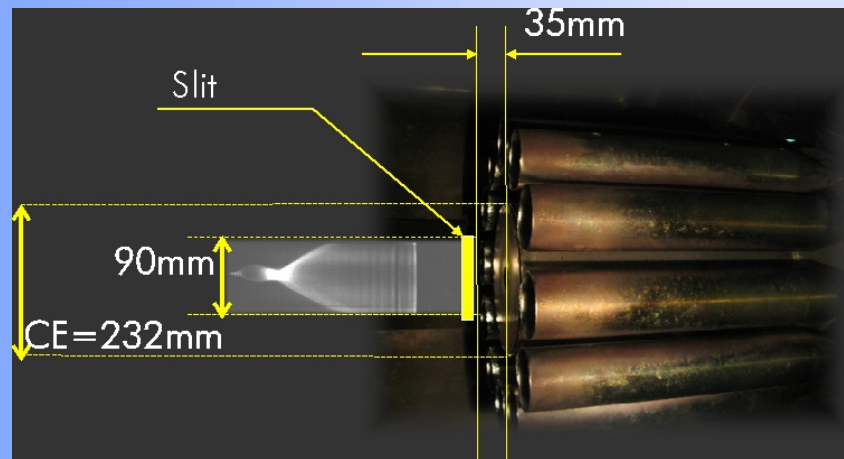
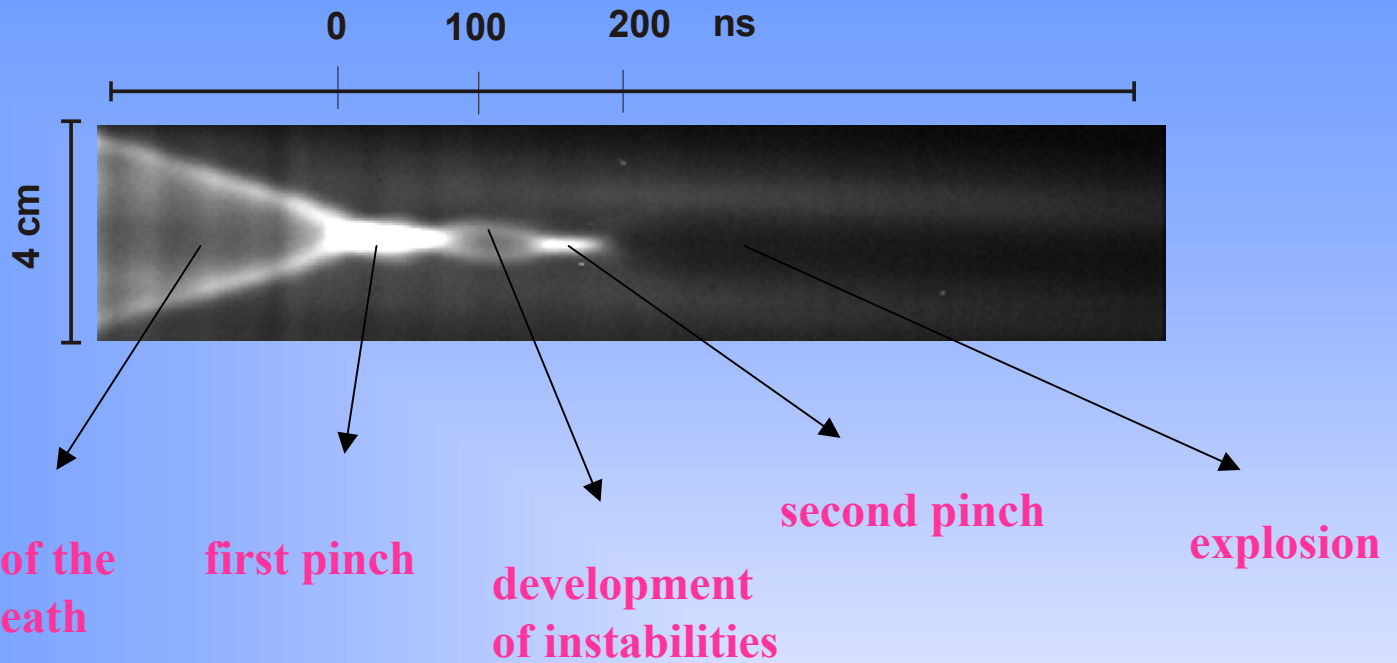
XUV frames - exposure time 2 ns, window 200-300 eV+above 600 eV



a-c pinch \varnothing 1-2 cm;
d - first expansion
e-f - second pinch
g-i explosion, dense structure
dense spherical structure

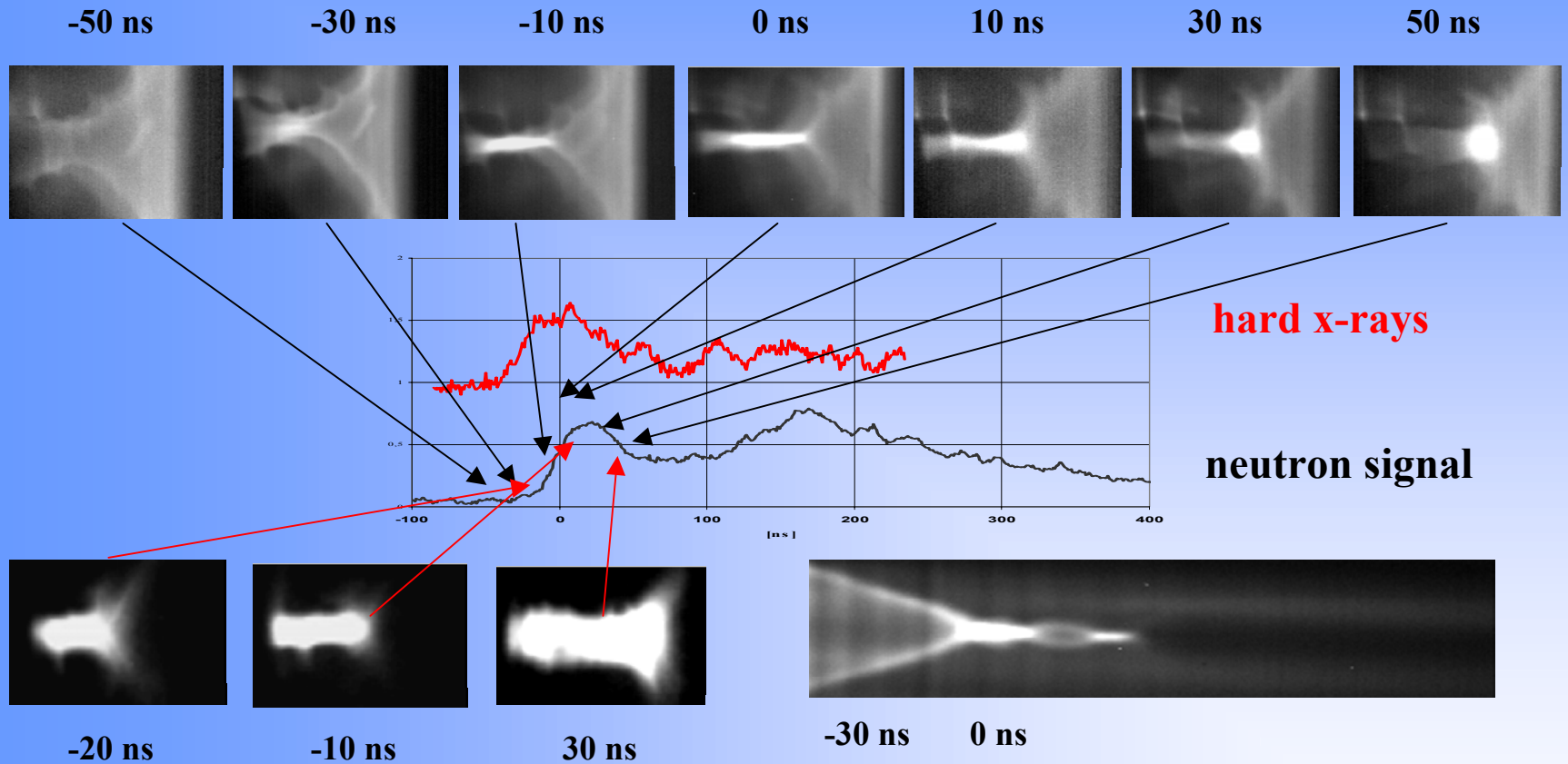


Visible streak-camera



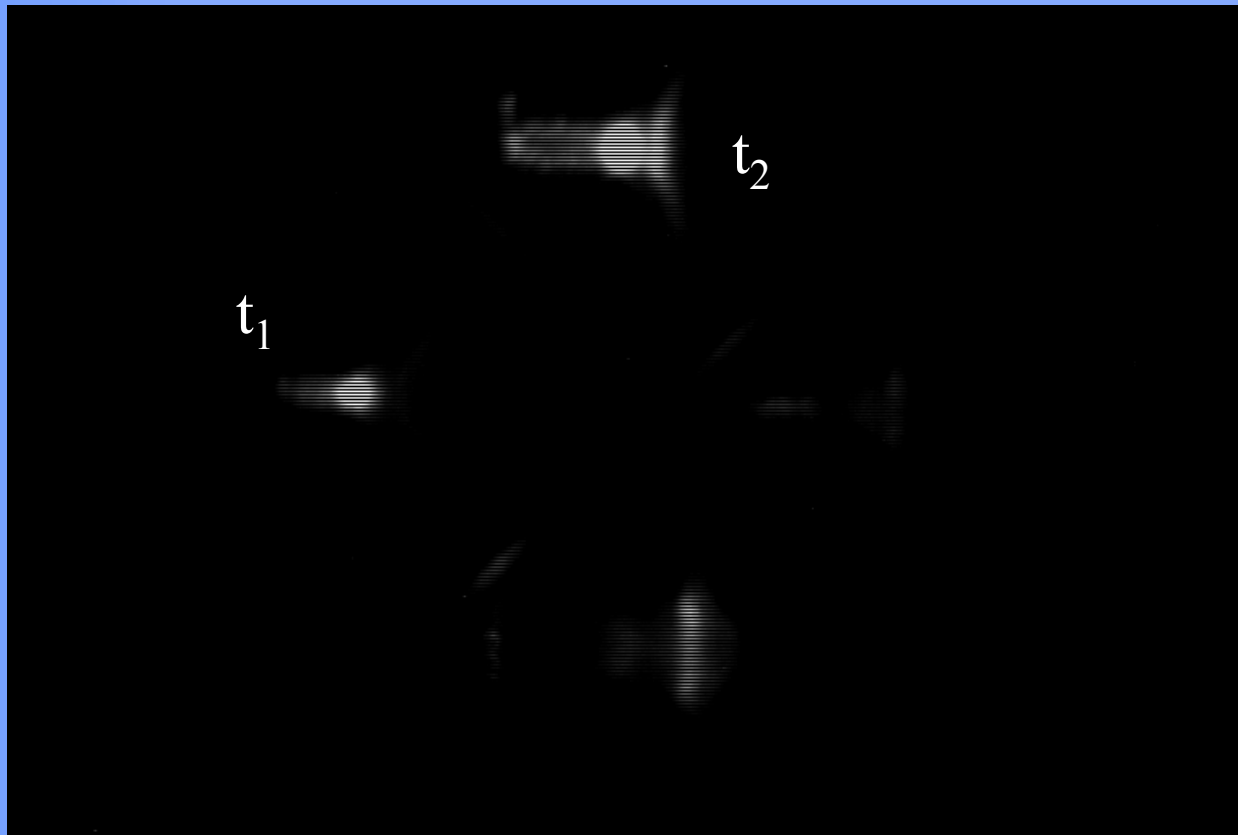


Correlation of neutron signals with frames *(first neutron pulse)*





XUV frames - exposure time 2 ns, window 200-300 eV+above 600 eV

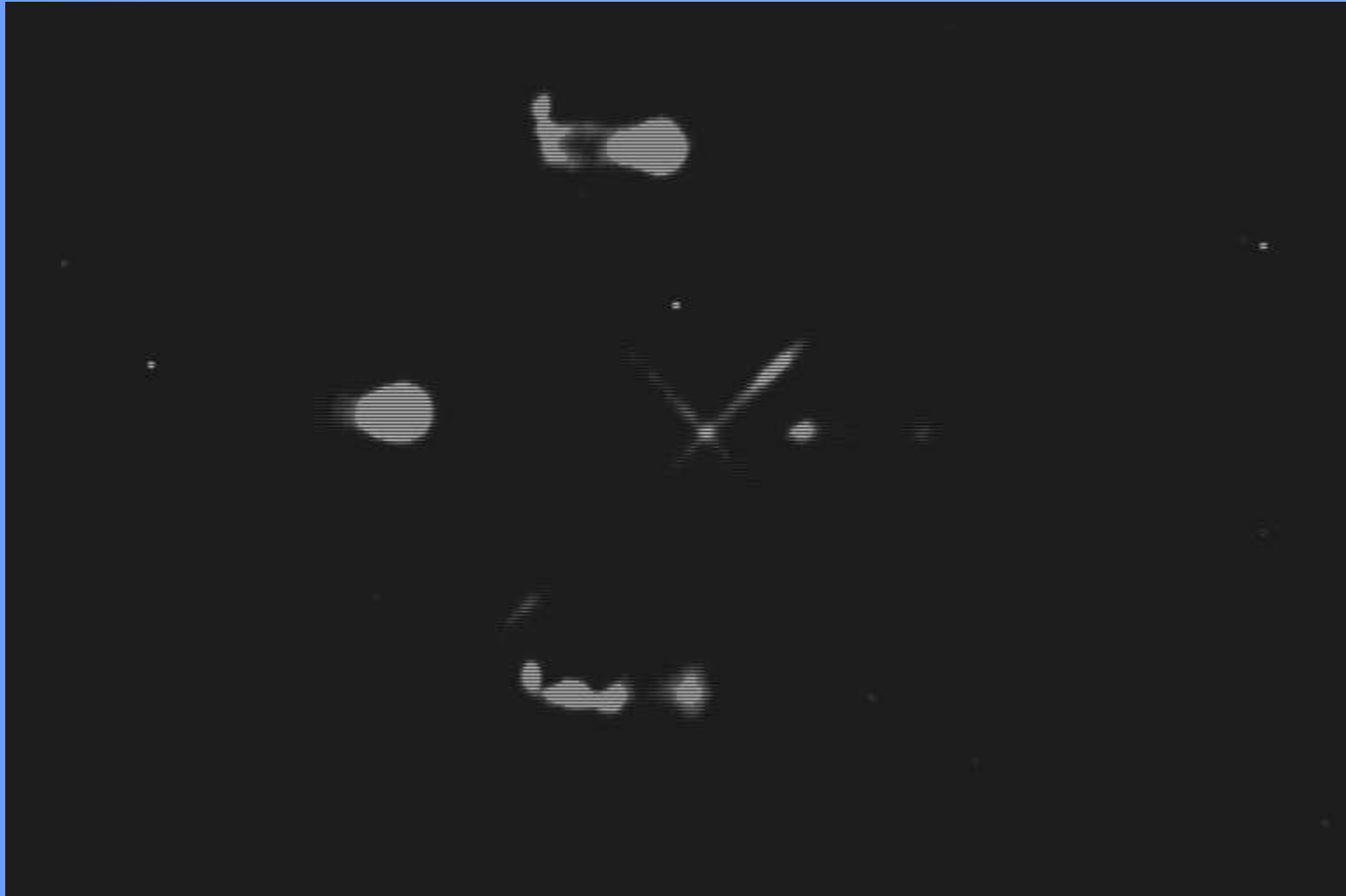


$t_2 - t_1 = 10 \text{ ns}$



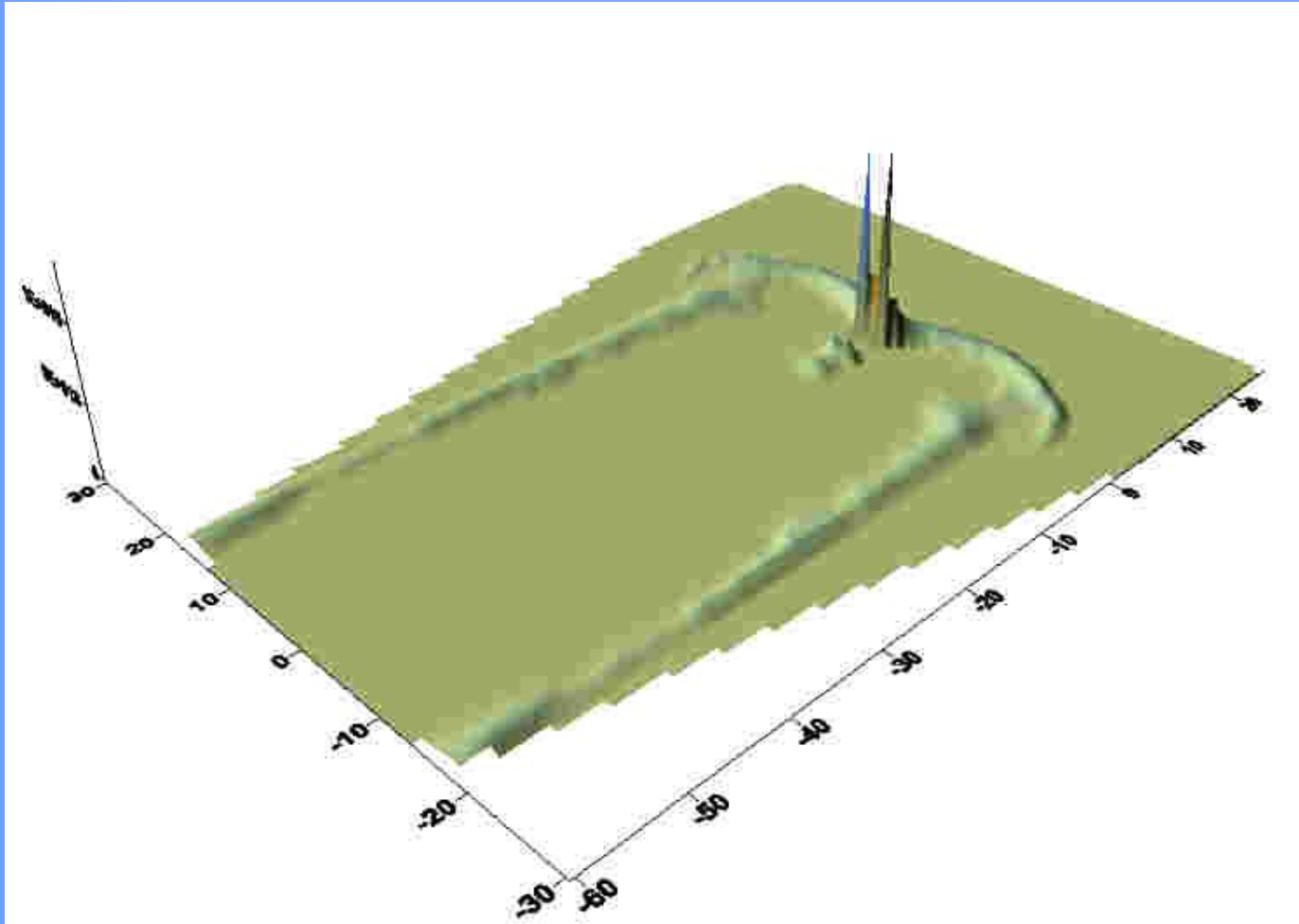


XUV frames - exposure time 2 ns, window 200-300 eV+above 600 eV



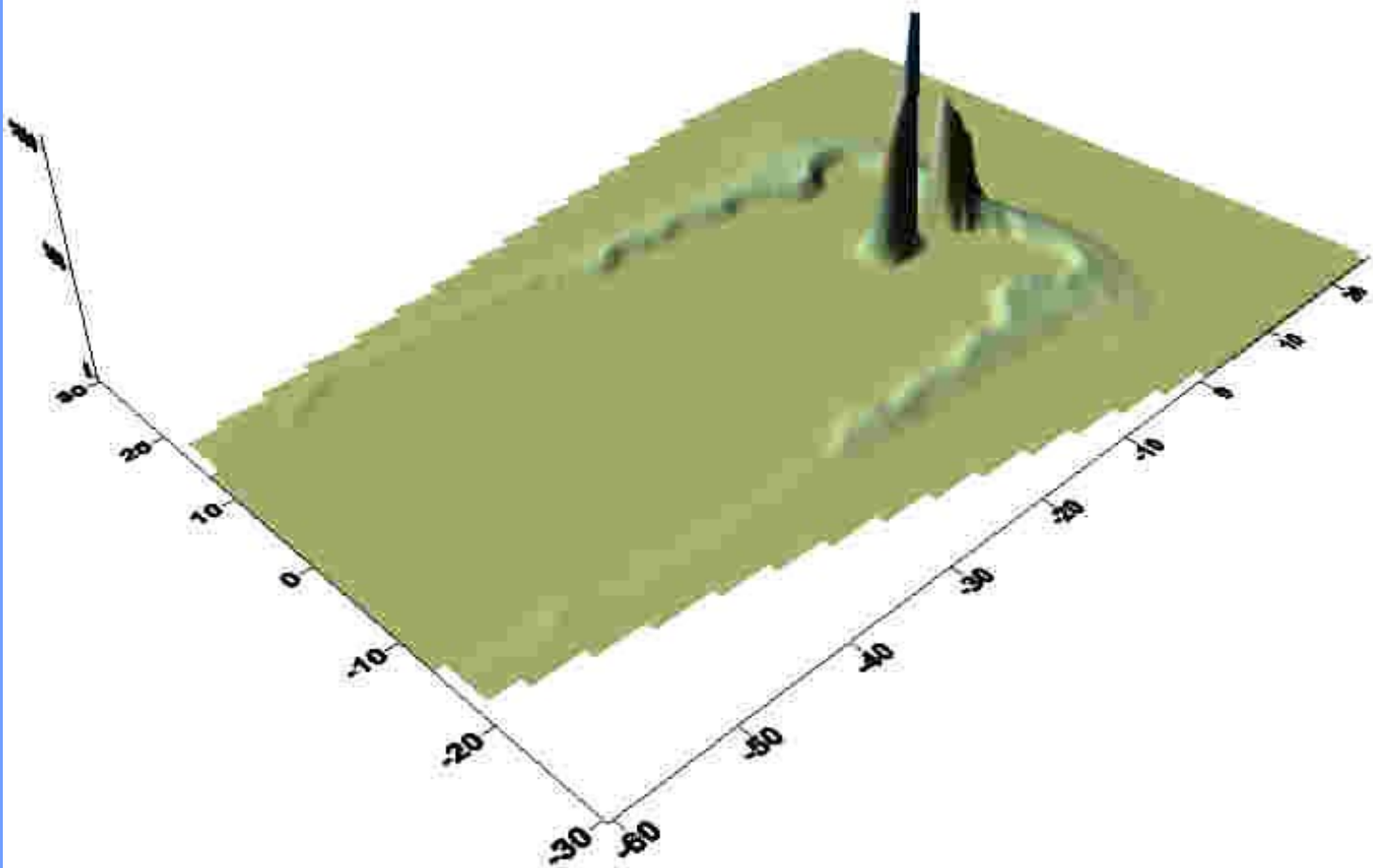
Calculated density

$t = 5,72 \mu s$



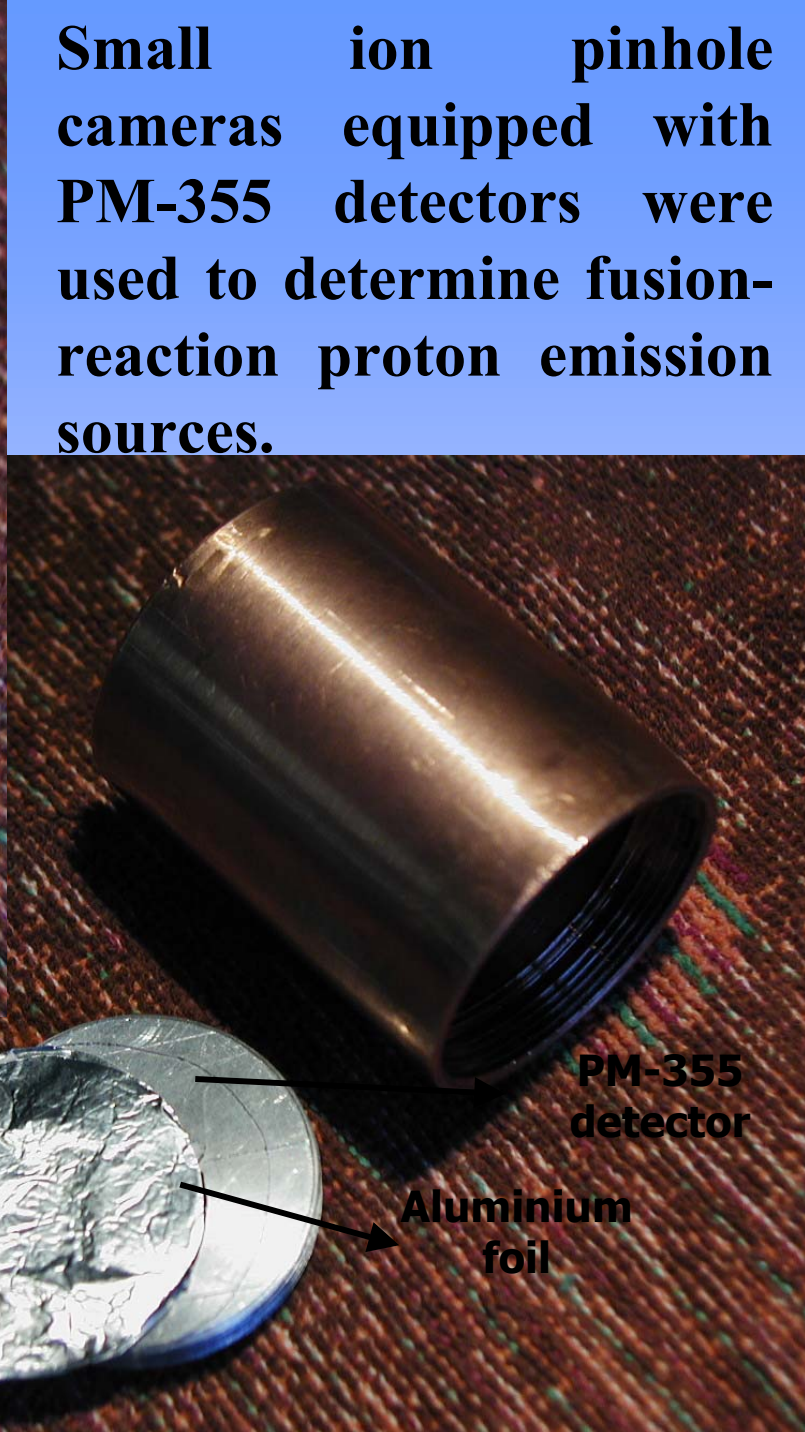
Calculated temperature of ions

$t = 5,72 \mu s$



obtained and presented by Sadowski, et al

Small ion pinhole cameras equipped with PM-355 detectors were used to determine fusion-reaction proton emission sources.

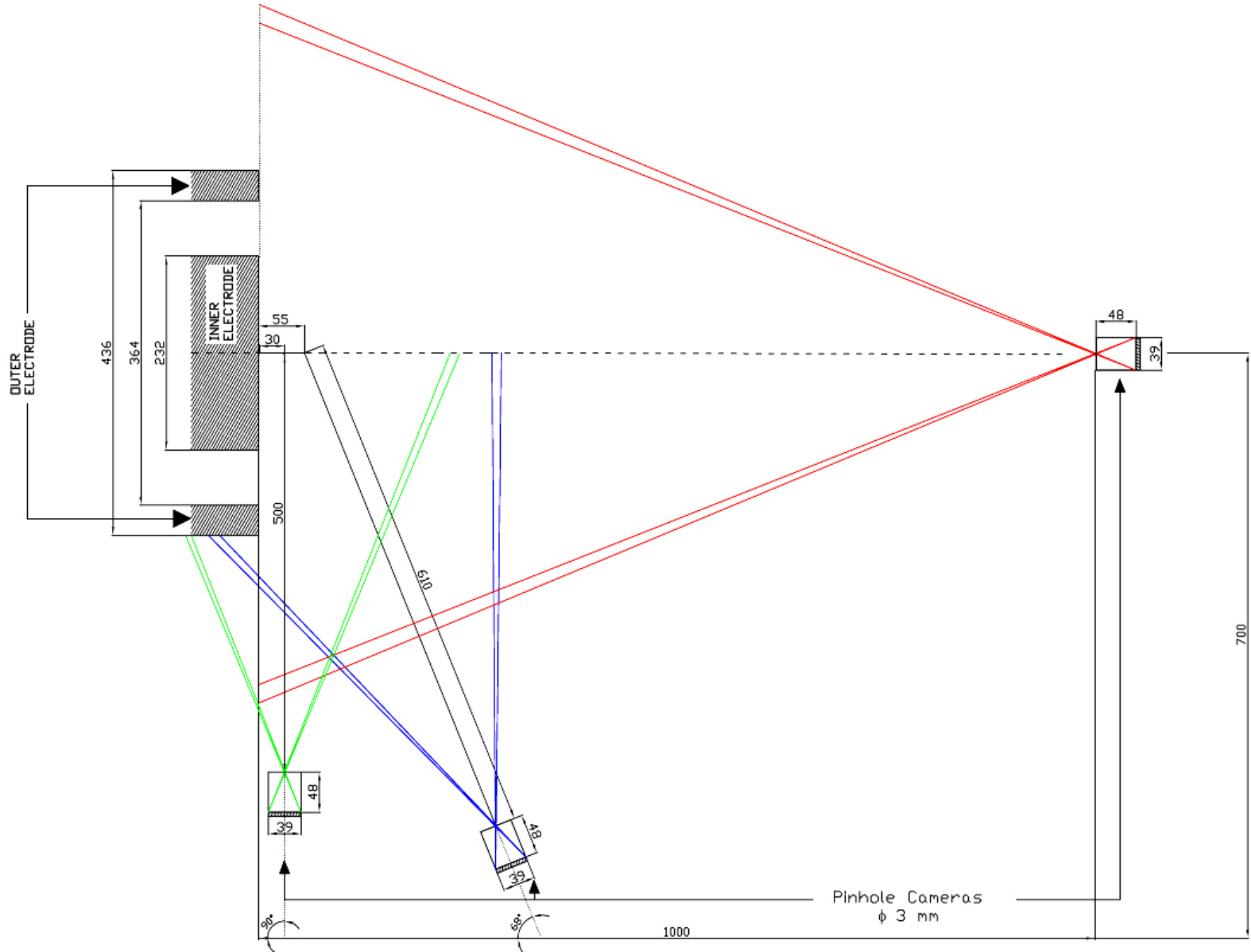


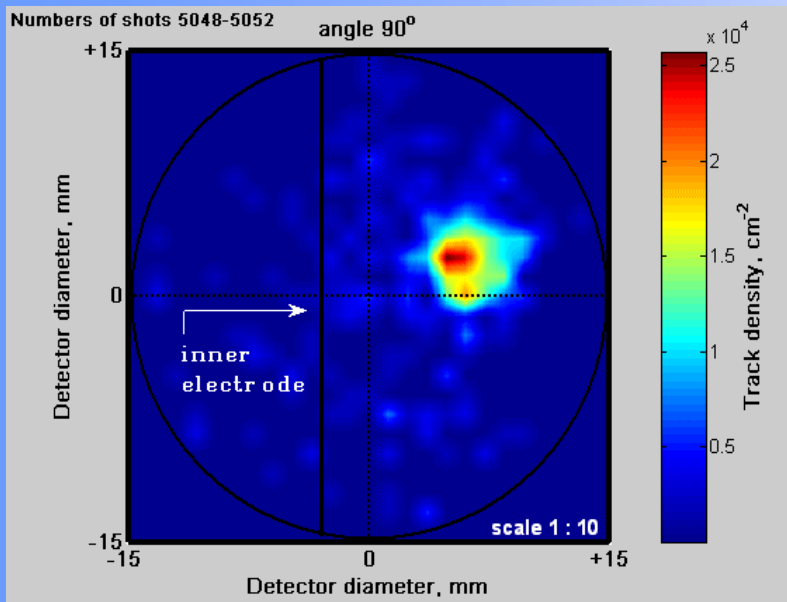
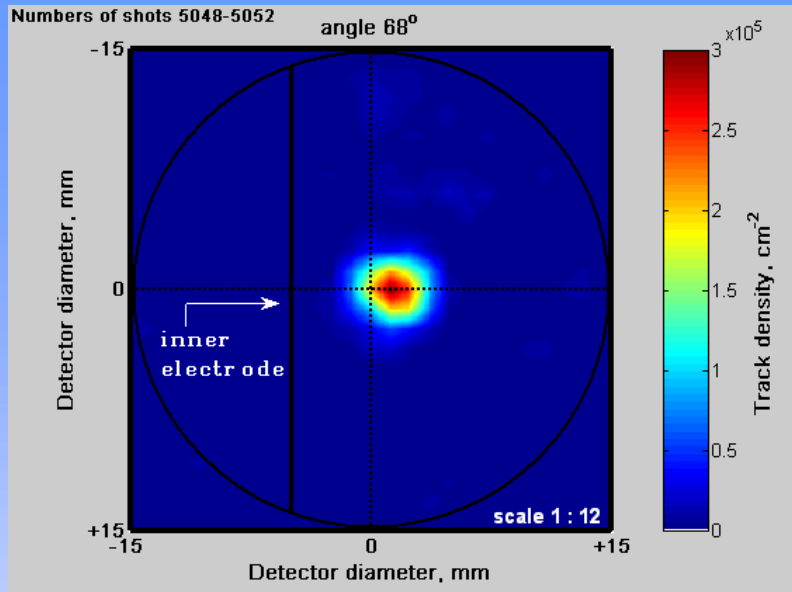
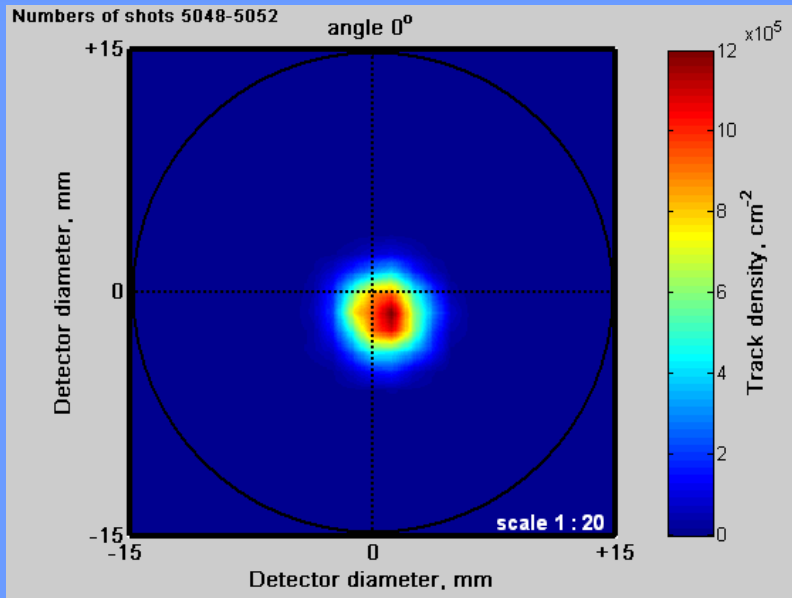
To eliminate fast primary deuterons the detector samples used in the cameras were covered with 80 μm thick Al-foils.

PM-355 detector

Aluminium foil

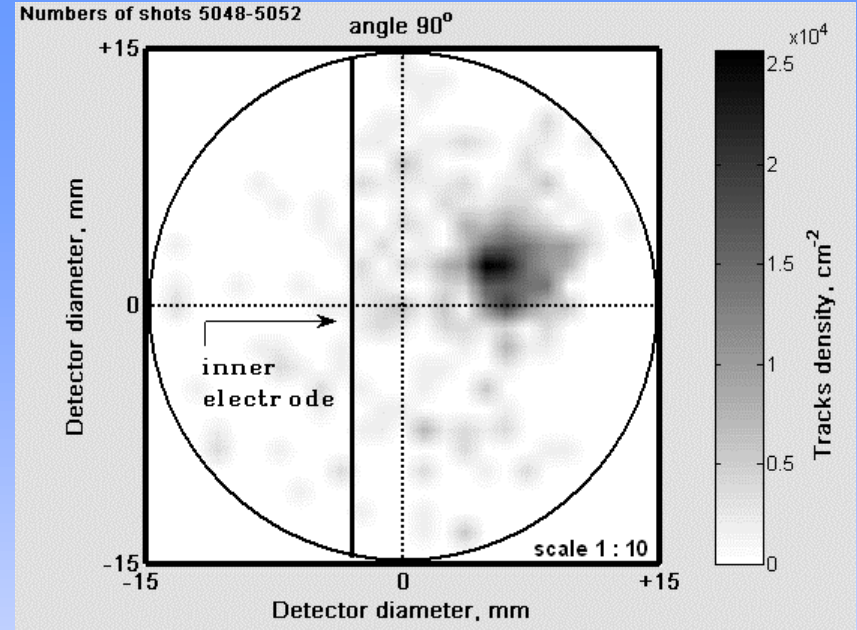
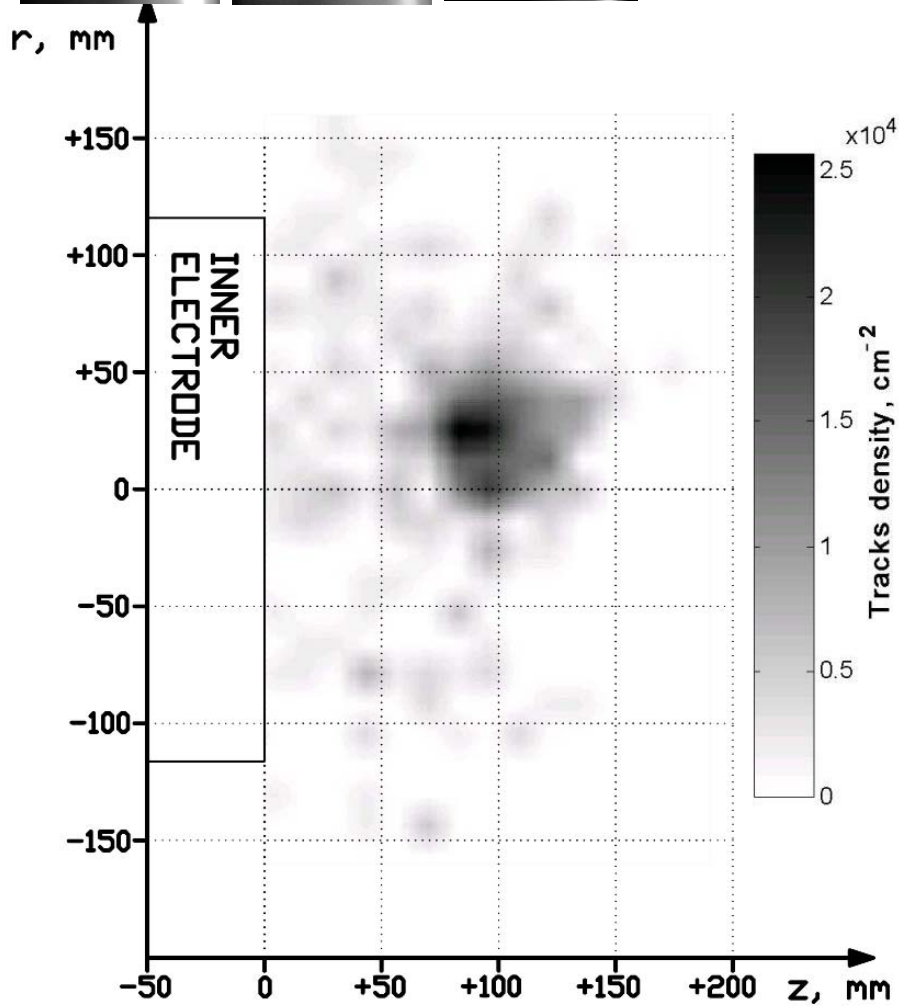
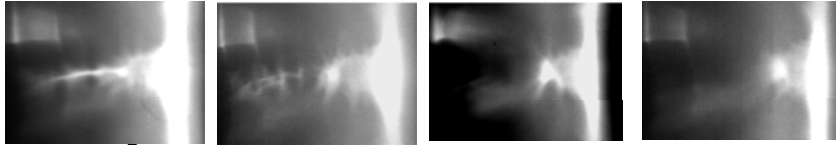
Positioning of ion-pinhole cameras within the PF-1000 facility during measurements of fusion-produced protons.





Images of fusion-proton emitting areas, as obtained after etching of the PM-355 detectors irradiated during five successive discharges within the PF-1000 facility (operated at $p_0 = 4$ Torr D_2 , $U_0 = 31$ kV).



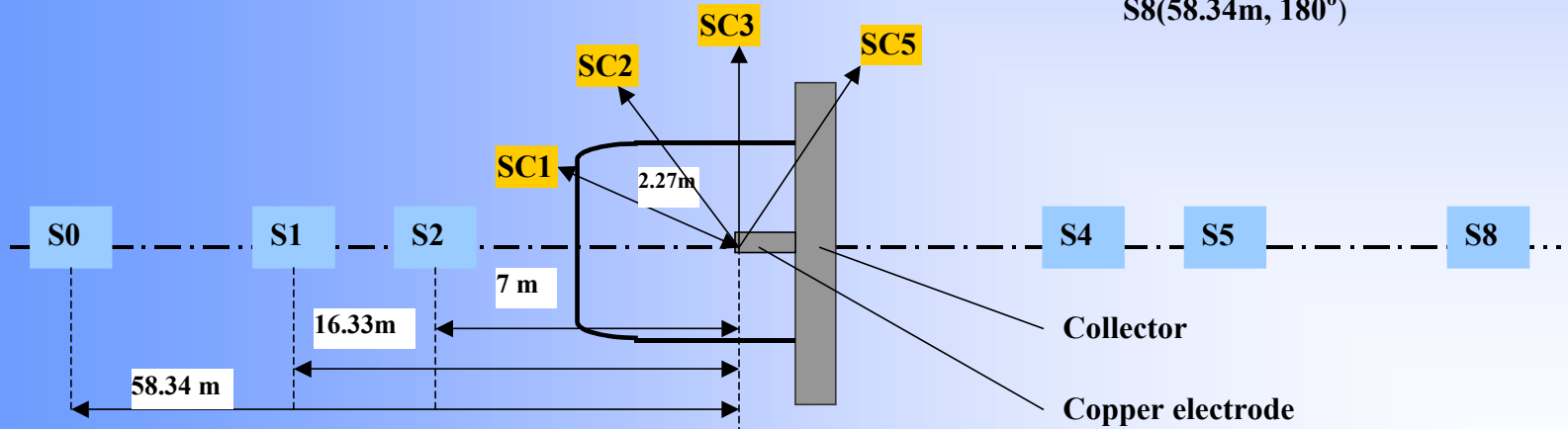


Example of the image of the fusion-produced protons, as recorded upon the detector placed at 90° to the z-axis in the PF-1000 facility.

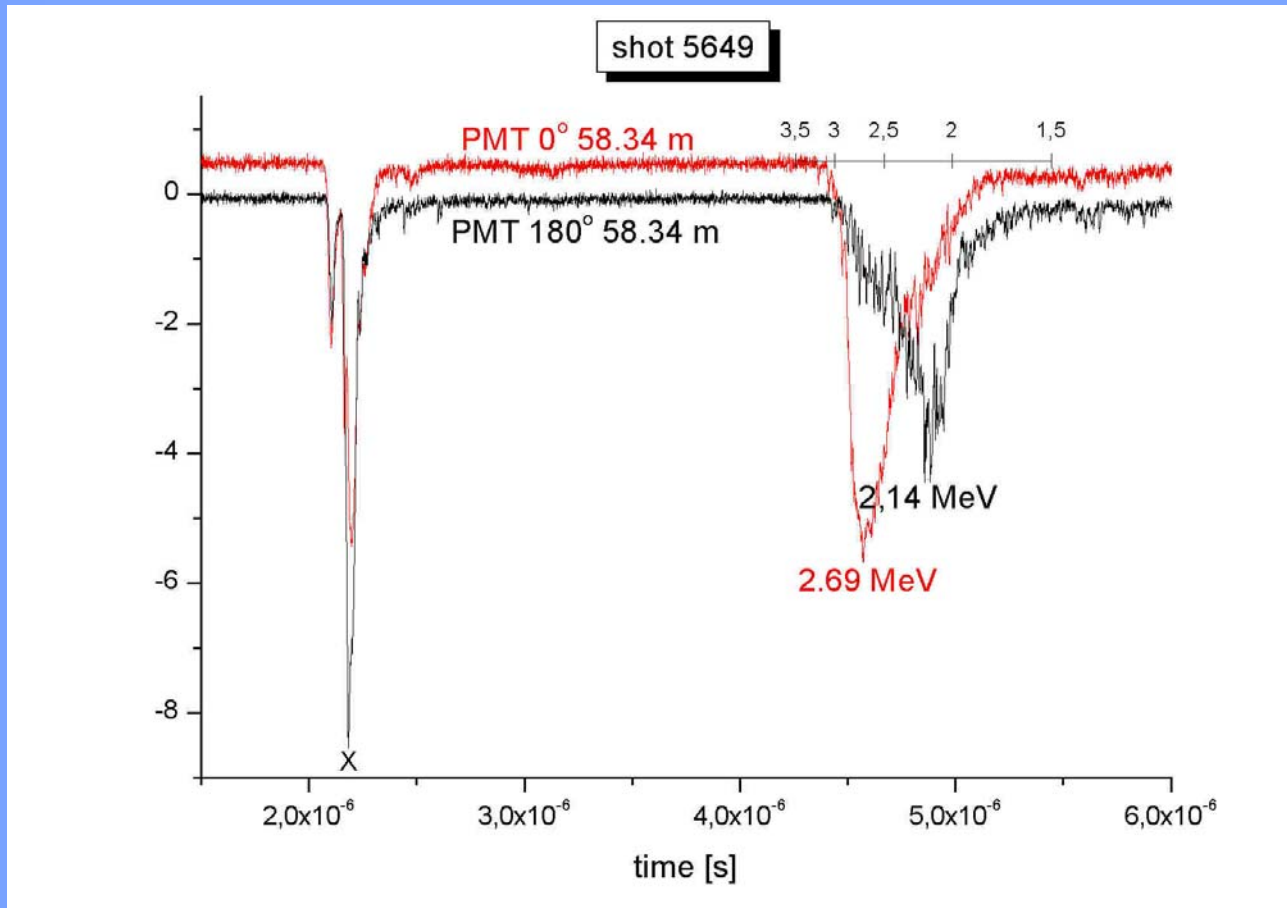


Activation silver counters:
SC1(30°), SC2(60°),
SC3(90°), SC5(150°)

Scintillator PMT detectors:
S0(58.34m, 0°), S1(16.33m, 0°),
S2(7m, 0°), S4(7m, 180°), S5(17m, 180°),
S8(58.34m, 180°)



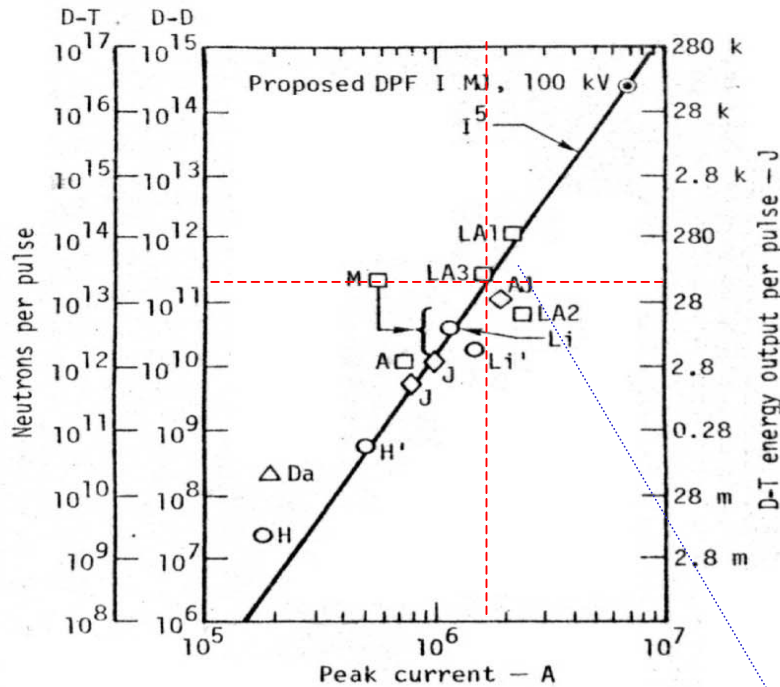
TOF Measurement



Results of TOF measurements

| Shot number | Y_n $L_1(90^\circ)$ | $t_n(0^\circ)$ [μs] | $t_n(180^\circ)$ [μs] | $\Delta t = t_n(180^\circ) - t_n(0^\circ)$ [μs] | E_b [keV] |
|-------------|--------------------------|-------------------------------------|---------------------------------------|---|-------------|
| 5544 | $2.03 \cdot 10^{11}$ | 4.734 | 5.055 | 0.321 | 70.0 |
| 5566 | $1.49 \cdot 10^{11}$ | 4.615 | 5.035 | 0.420 | 120 |
| 5569 | $1.76 \cdot 10^{11}$ | 4.643 | 4.965 | 0.322 | 70.4 |
| 5575 | $1.92 \cdot 10^{11}$ | 4.509 | 4.789 | 0.280 | 53.2 |
| 5592 | $1.34 \cdot 10^{11}$ | 4.623 | 4.911 | 0.288 | 56.3 |
| 5605 | $2.28 \cdot 10^{11}$ | 4.770 | 5.158 | 0.388 | 102 |
| 5620 | $1.14 \cdot 10^{11}$ | 4.860 | 5.147 | 0.287 | 55.9 |
| 5649 | $1.55 \cdot 10^{11}$ | 4.573 | 4.874 | 0.301 | 61.5 |





A “historical” experimental scaling law for neutron yield as a function of the total discharge current (assembled in 1975).

Legend

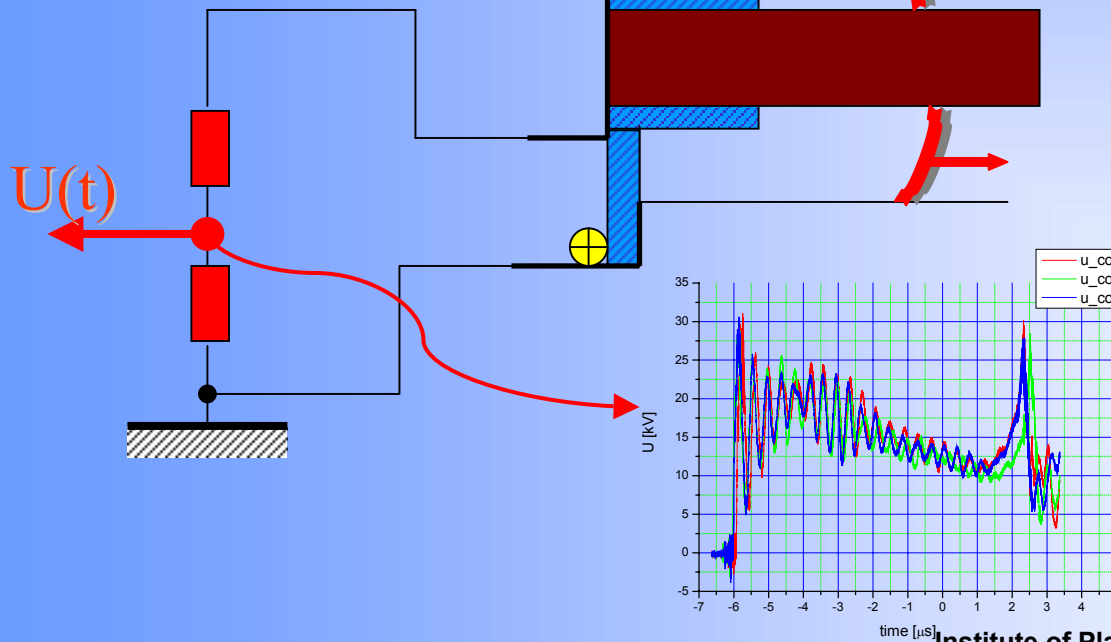
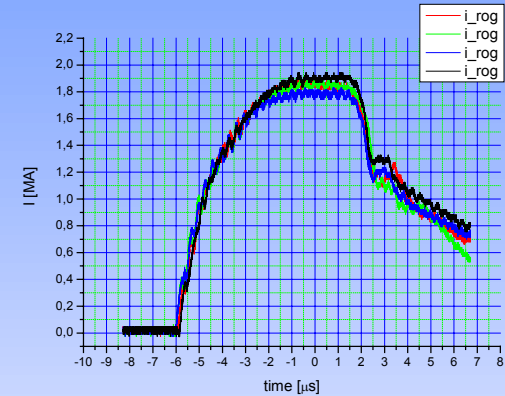
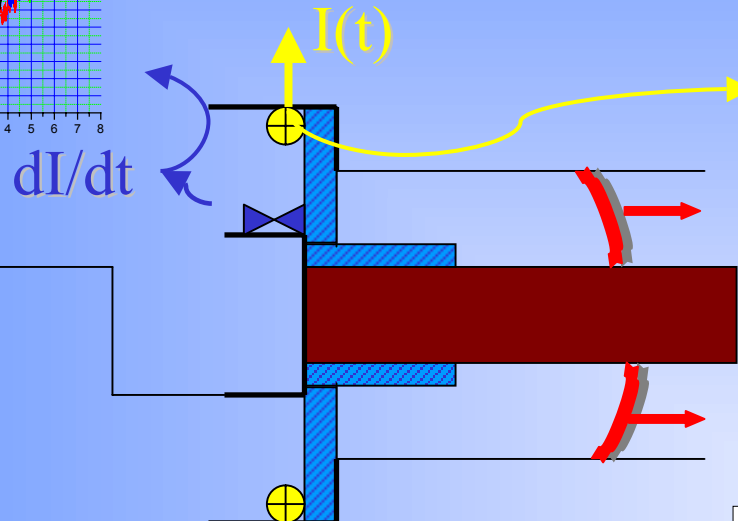
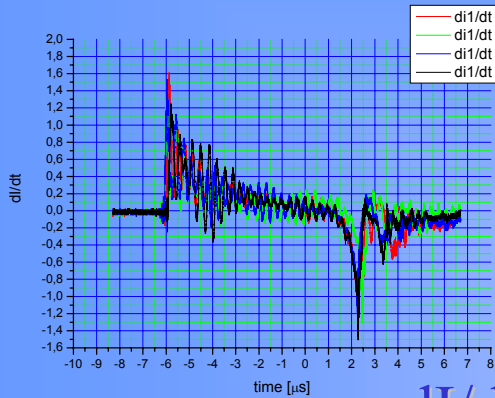
- AJ Aerojet Nucleonics. 250 kJ, 20 kV, 320 μ F.
- Da Darmstadt. 0.34 - 1.35 kJ;]0 - 20 kV.
- H Hoboken. Electrode structure is identical to that of Darmstadt group.
- H' Hoboken. About 5 kJ.
- A^E Aerospace Corporation.
- J Julich. 25 kJ; 40 kV.
- Li Limeil. 96 kJ, 40 kV.
- Li' Limeil. Plasma focus driven by explosive generator.
- LA¹ Los Alamos. DPF-6; 420 kJ.
- LA² Los Alamos. DPF-5; 120 kJ.
- LA³ Los Alamos. DPF-6; 210 kJ.
- M Moscow. $Y \rightarrow 10^{10}$ to 10^{11} DD neutrons; I = 1 MA.

**PF-1000, 1,8 MA,
Y \approx 3·10¹¹ n/shot,
E=480 kJ**





Measurements of Current and Voltage



$$U_b = 27 \text{ kV}, E_b = 480 \text{ kJ},$$

$$p = 3,5 \text{ Torr}$$

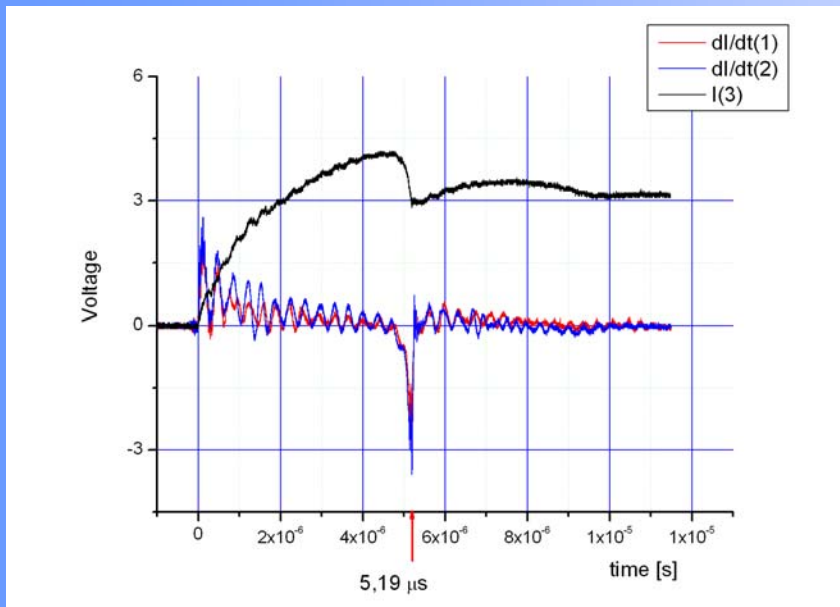
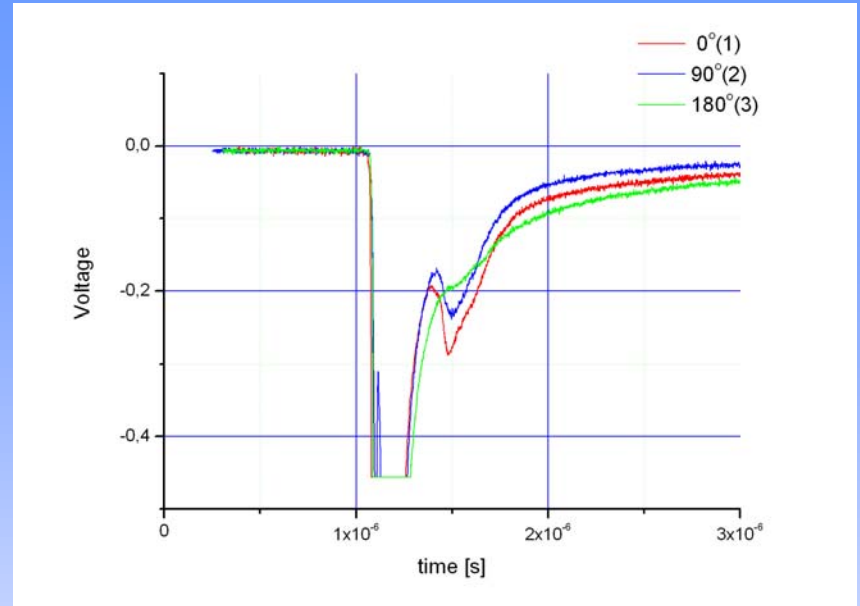
$$Y = 5 \cdot 10^{10} - 3 \cdot 10^{11}$$



SHOT 6814

2,5 Tr 29 kV

| | | |
|----|---------|---------------------|
| L1 | 124 286 | $3,057 \times 10^6$ |
| L2 | 89152 | $3,036 \times 10^6$ |
| L3 | 72593 | $4,192 \times 10^6$ |
| L4 | 67608 | $4,777 \times 10^6$ |
| L5 | 46426 | $6,583 \times 10^6$ |



SHOT 6817 2 Tr 29 kV

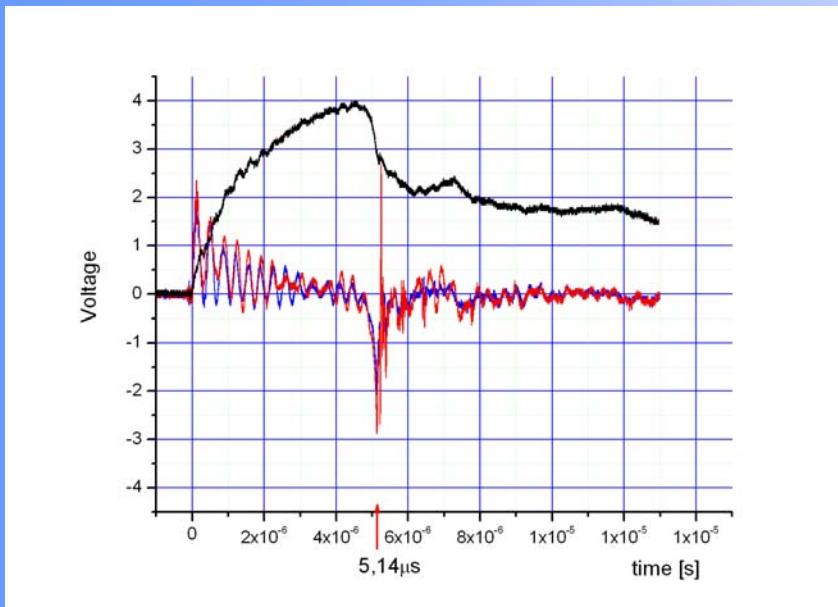
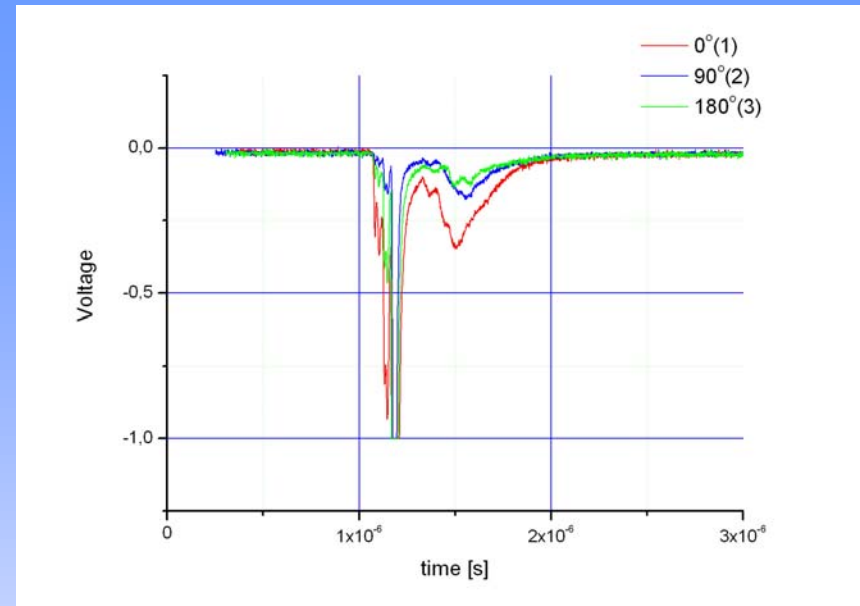
L1 102078 $3,057 \times 10^6$

L2 74183 $3,036 \times 10^6$

L3 57928 $4,192 \times 10^6$

L4 47904 $4,777 \times 10^6$

L5 35016 $6,583 \times 10^6$



SHOT 6820 2,75 Tr 29 kV

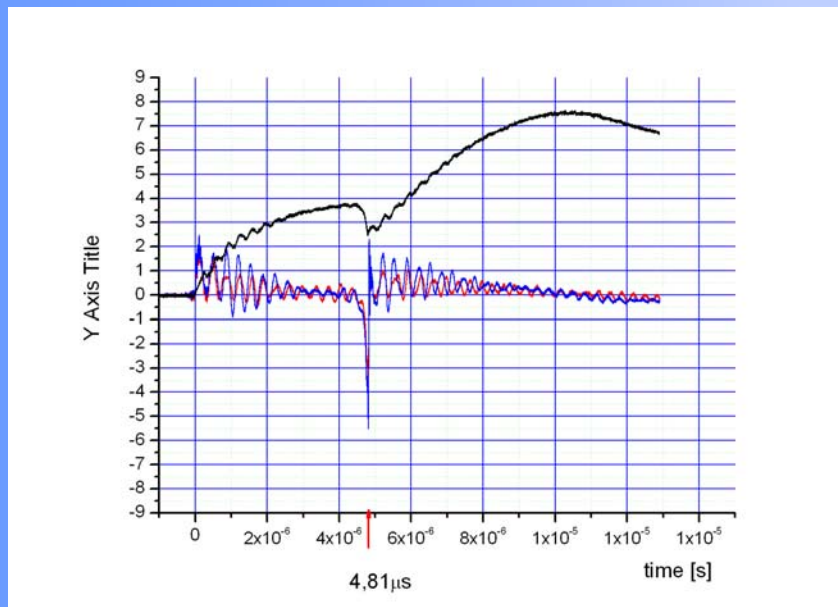
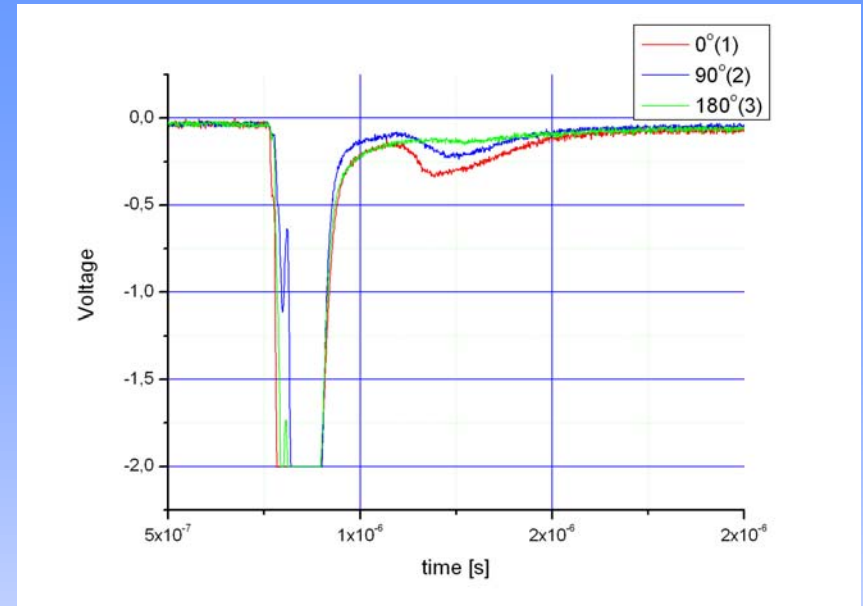
L1 163160 $3,057 \times 10^6$

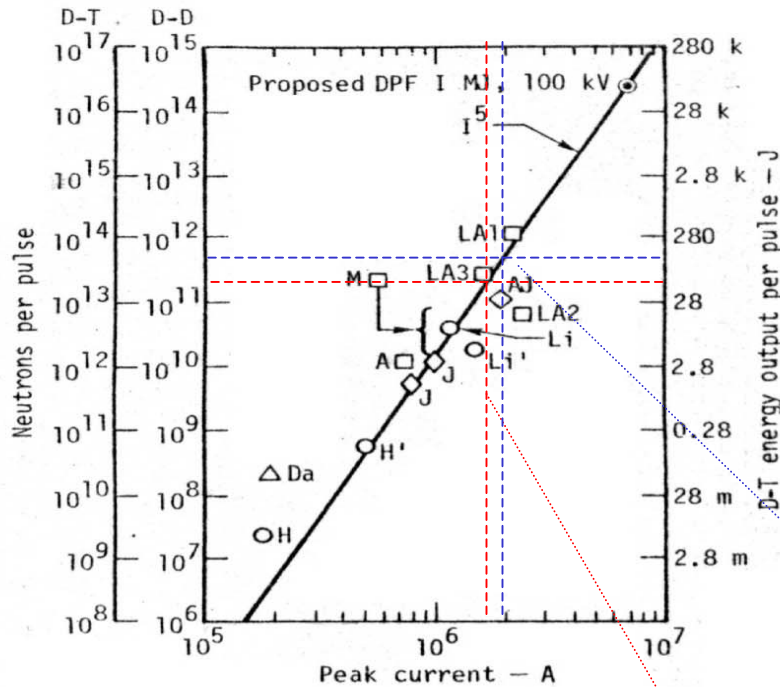
L2 106836 $3,036 \times 10^6$

L3 96329 $4,192 \times 10^6$

L4 93122 $4,777 \times 10^6$

L5 57110 $6,583 \times 10^6$





A “historical” experimental scaling law for neutron yield as a function of the total discharge current (assembled in 1975).

Legend

- AJ Aerojet Nucleonics. 250 kJ, 20 kV, 320 μ F.
- Da Darmstadt. 0.34 - 1.35 kJ;]0 - 20 kV.
- H Hoboken. Electrode structure is identical to that of Darmstadt group.
- H' Hoboken. About 5 kJ.
- A^E Aerospace Corporation.
- J Julich. 25 kJ; 40 kV.
- Li Limeil. 96 kJ, 40 kV.
- Li' Limeil. Plasma focus driven by explosive generator.
- LA¹ Los Alamos. DPF-6; 420 kJ.
- LA² Los Alamos. DPF-5; 120 kJ.
- LA³ Los Alamos. DPF-6; 210 kJ.
- M Moscow. $Y \rightarrow 10^{10}$ to 10^{11} DD neutrons; I = 1 MA.

PF-1000, 1,95 MA,

$Y \approx 6 \cdot 10^{11}$ n/shot,

E=550 kJ

PF-1000, 1,8 MA,

$Y \approx 3 \cdot 10^{11}$ n/shot,

E=480 kJ



Question for future

- Determination of parameters of the dense plasma structure in the head of the pinch
 - **role of outflow**
 - role of dissipation processes of magnetic field energy into a pinch plasma
 - **nature of neutron generation**
-

Correct neutron measurements

Measurements of a current flowing in a pinch



Diagnositics

$$P = \frac{N_D n_D}{4} \cdot \langle \sigma v \rangle \tau$$

Interferometry !!;

Streak camera

$$Y_n = l \cdot P \propto \alpha \frac{l}{a} I^4 \cdot \frac{\langle \sigma v \rangle}{T^{5/2}}$$

Activation Measurements

(anizotropy !!)

Method of calibration!

PMT

TOF (spectra)

Current probes

Soft X-ray Measurements

(D+Ar or D+Kr)



Interferometry for PF-1000

Mach-Zenhderr

Laser output specyfication

16 frames, 60 ns between frames

Max. Pulse energy, mJ

At 1053 nm 1000

At 527 nm 450

At 351 nm 320

At 263 nm 160

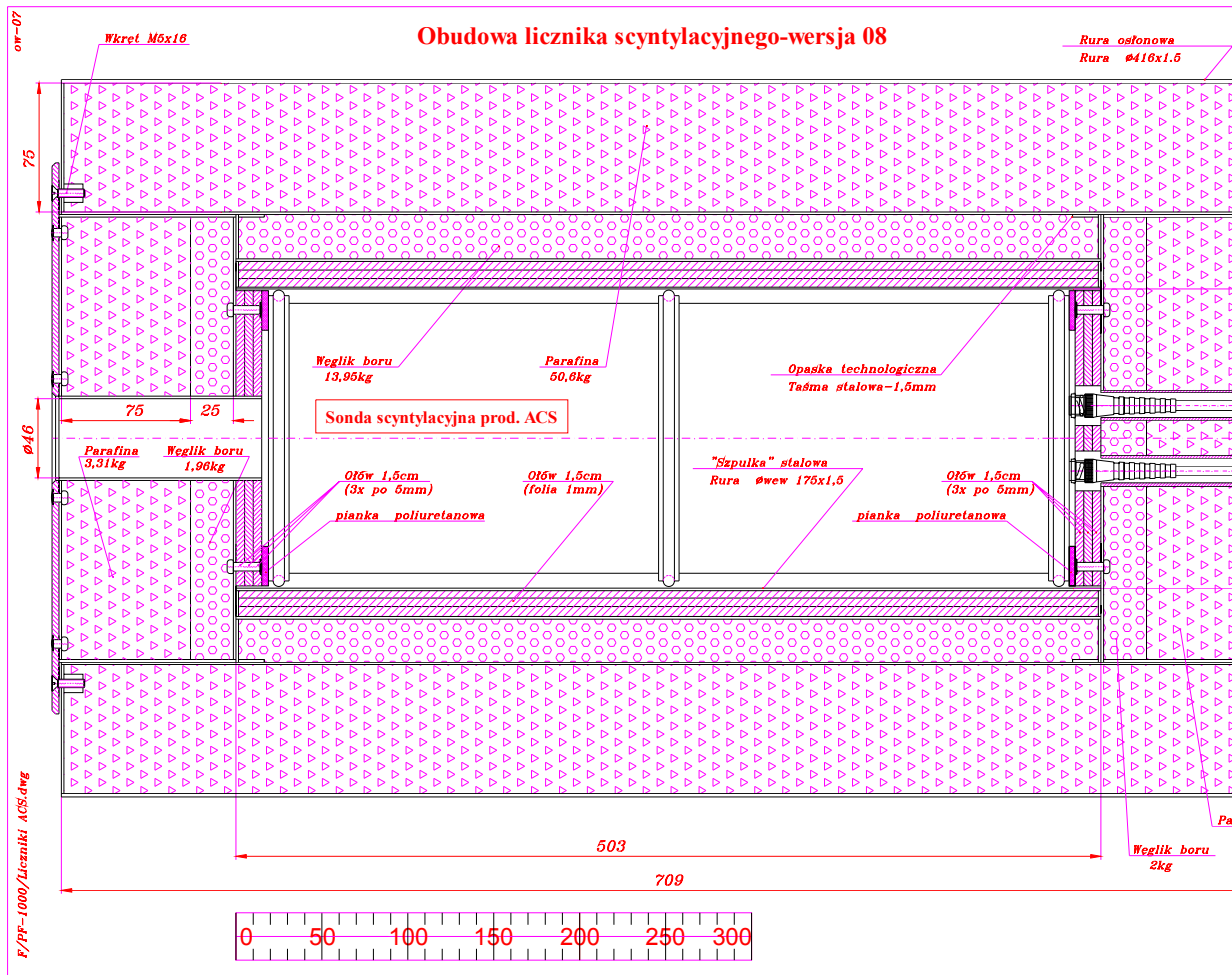
Pulse duration at 1053 nm (FWHM) < 1 ns

Optical pulse jitter +/-1 ns

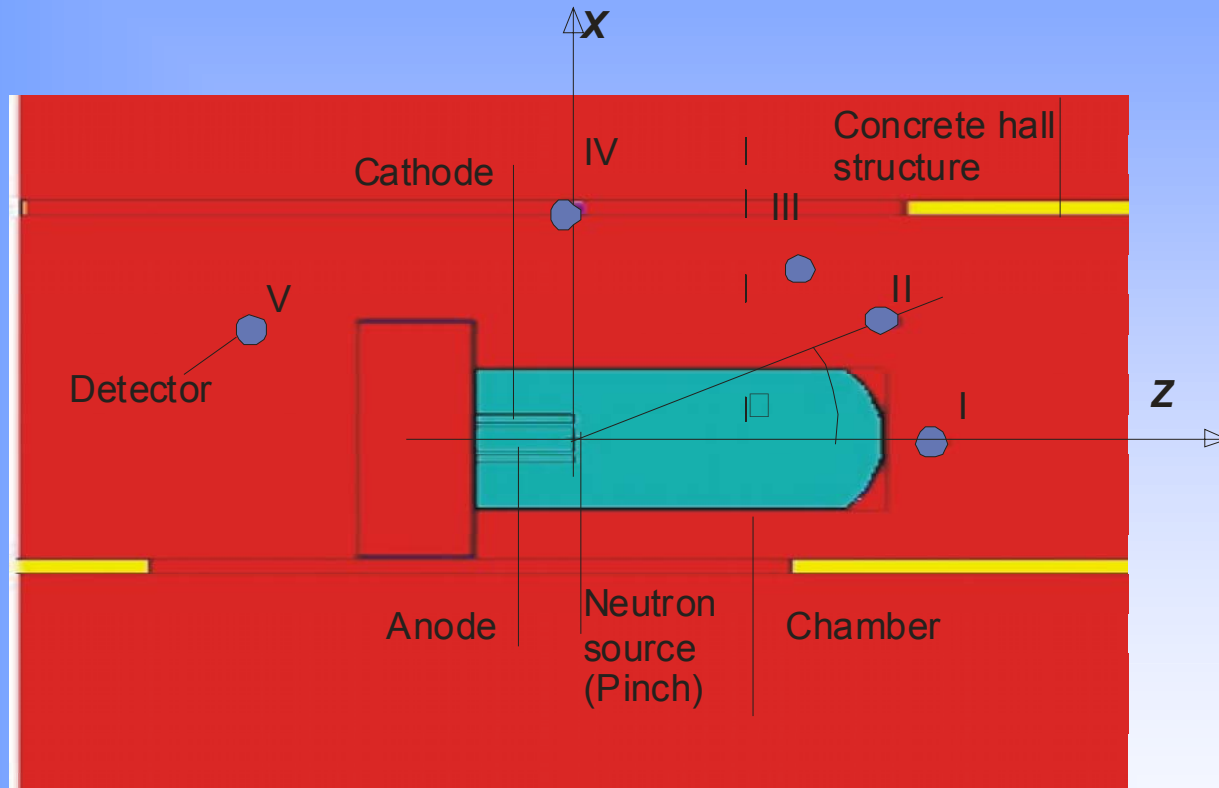
Beam divergence at 1053 nm (ful angle @ 1/e²) < 0.25 mrad

Beam diametr 12 mm



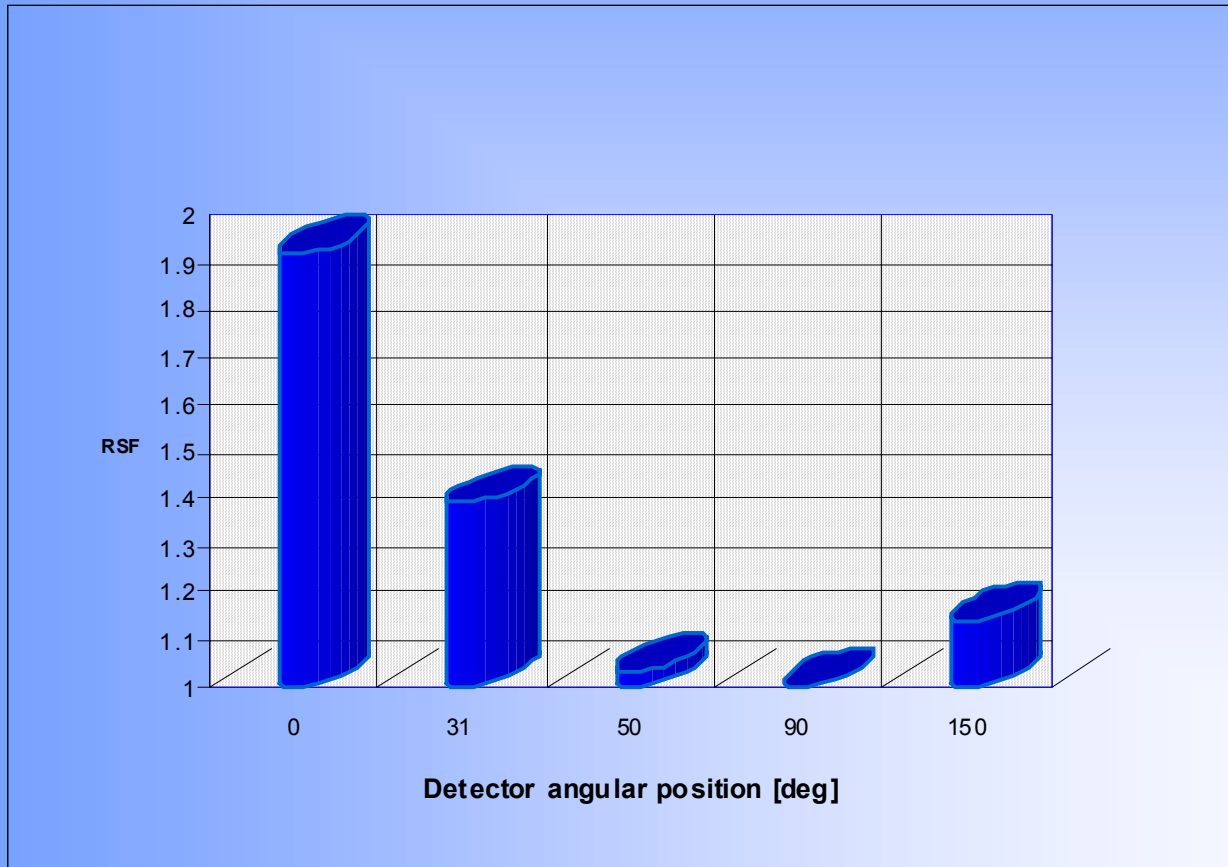


Cut view of MCNP geometry of PF-1000 facility.

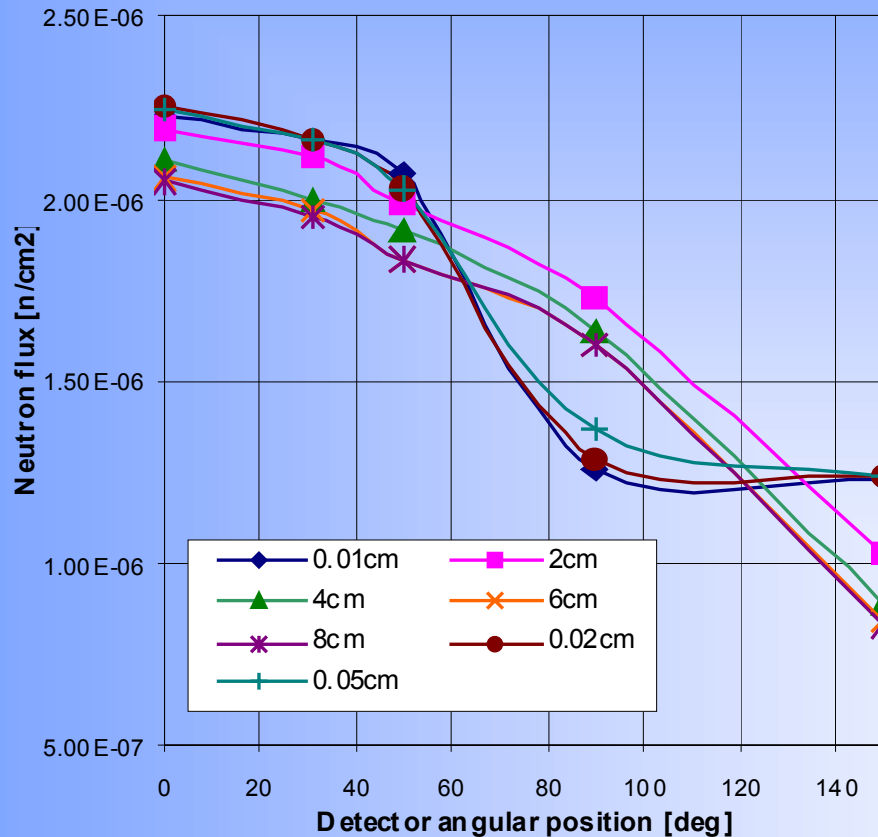


RSF (Response Scaling Factor) as a function of detector angular position.

$RSF = \text{Response}(2.5 \text{ MeV source}) / \text{Response}(\text{Am-Be source})$.



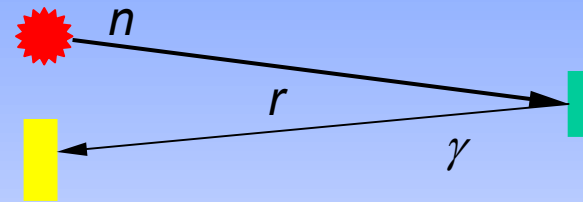
Thermal neutron flux as a function of detector position calculated for point 2.5 MeV neutron source located on 'Z' axis and distanced 0.1, 0.2, 0.5, 2, 4, 6 and 8 cm from the anode



Idea of the method

Fast neutron interactions

$(n, n'\gamma)$ $t_{\text{ch}} \sim 10^{-12}$ s



$$F = \frac{MN_A}{A} \cdot \langle \sigma \Phi \rangle \cdot (a\psi)$$

$$Y = \frac{MN_A}{A} \cdot \langle \sigma \Phi \rangle$$

$(n, \gamma), (n, n'), (n, 2n)$
 $(n, p), (n, \alpha), (n, \beta)$ $T_{1/2}$ s

$$A_0 = \frac{MN_A}{A} \cdot \langle \sigma \Phi \rangle \cdot (a\psi) \eta (1 - e^{-\lambda T})$$

$$\langle \sigma \Phi \rangle = \int \sigma(E) \Phi(E) dE$$

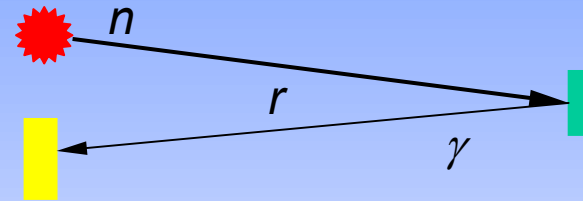


Procedure of calibration

1.
$$\langle \sigma \Phi \rangle = \frac{A_0}{(a\psi)M(N_A/A)\eta(1-e^{-\lambda T})}$$

Calibration source with defined S

$$S = \frac{\langle \sigma(E)\Phi(E) \rangle_{\text{exp}}}{K_{\text{exp}}}, \begin{bmatrix} n \\ s \end{bmatrix}$$



2. MCNP modelling including:

defined calibration source;

all masses surrounding the source;

defined samples

$$S = \frac{\langle \sigma(E)\Phi(E) \rangle_{\text{cal}}}{K_{\text{cal}}}, \begin{bmatrix} n \\ s \end{bmatrix}$$

3. MCNP modelling including:

DD neutron source (plasma) Y_n ;

all masses surrounding the source;

defined samples

$$Y_n = \frac{\langle \sigma(E)\Phi(E) \rangle_{DD}}{K_{DD}}, \begin{bmatrix} n \\ s \end{bmatrix}$$



Neutron Activation Diagnostic

New Foil Project

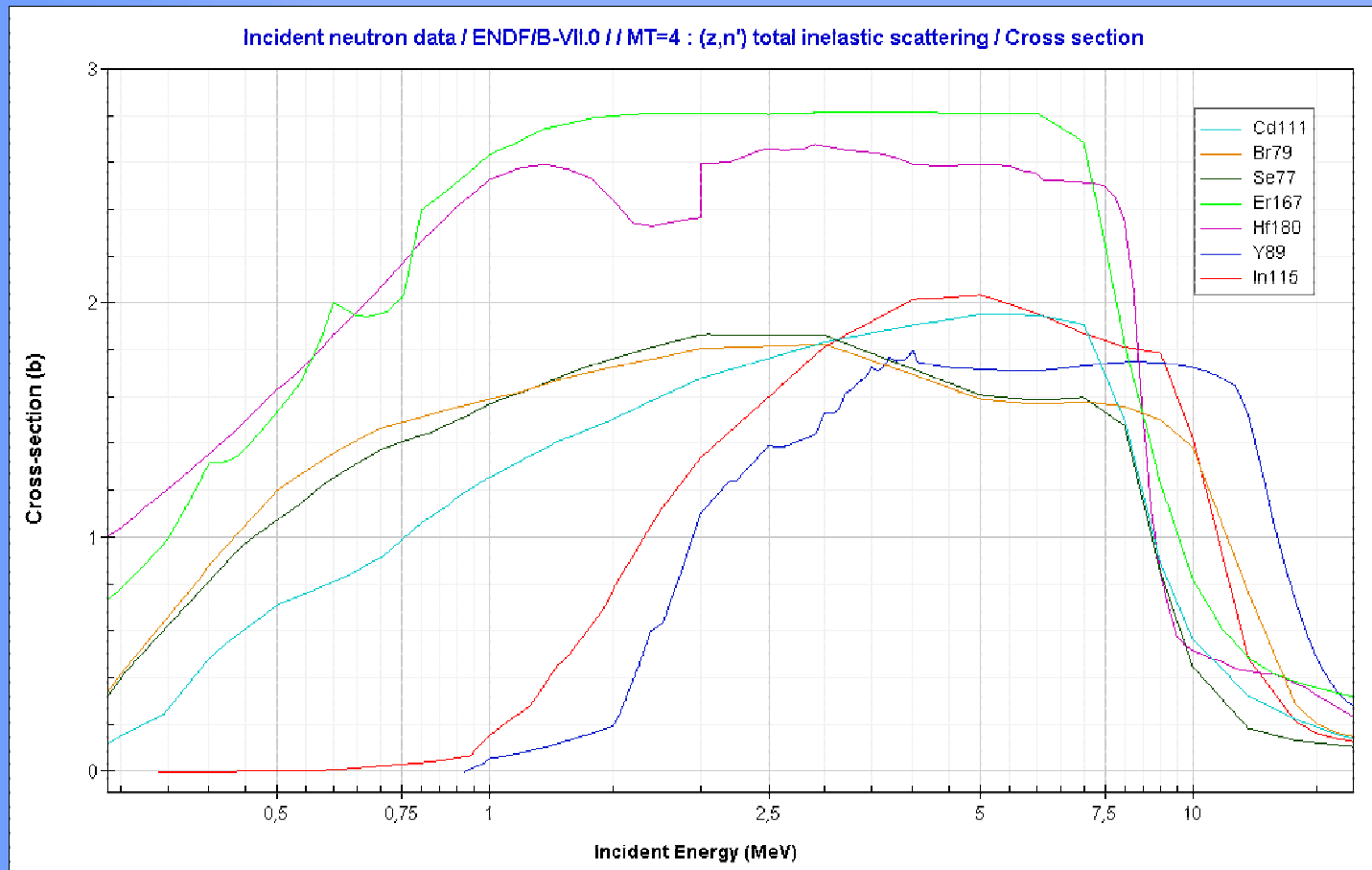
1. Selection of an appropriate set of neutron activation foils, depending on the anticipated measurement conditions.

| Reaction | E _γ [keV] | Max. line En. Effic (C19 cal) | Daughter T _{1/2} | σ _{2.45} [barn] | Parent abundance ratio (Θ) | Sensitive for thermal neutrons (S _{th}) | Relative mass ratios | | | | |
|---|---------------------------|-------------------------------|---------------------------|--------------------------|----------------------------|---|----------------------|-----|-----|-----|-----|
| ²⁷ Al (n,γ) ²⁸ Al | 1779(1) | 0.6 · 10 ⁻³ | 2.2 m | 0.4 | 1 | Yes | 20% | 37% | 18% | 22% | 27% |
| ²⁷ Al (n,p) ²⁷ Mg | 844(0.718), 1014 | 1.6 · 10 ⁻³ | 9.5 m | 1.5E-5 | 1 | No | | | | | |
| ¹⁸⁰ Hf (n,n') ^{180m} Hf | 215, 332(0.941), 443, 501 | 4.4 · 10 ⁻³ | 5.5 h | 2.7 | 0.3508 | No | 20% | 0% | 18% | 0% | 26% |
| ¹⁸⁰ Hf (n,γ) ¹⁸¹ Hf | 133, 346, 482(0.805) | 2.9 · 10 ⁻³ | 42.4 d | 0.03 | 0.3508 | Yes | | | | | |
| ¹¹¹ Cd (n,n') ^{111m} Cd | 151, 245(0.94) | 6.2 · 10 ⁻³ | 48.5 m | 1.76 | 0.128 | No | | | | | |
| ¹¹⁶ Cd (n,γ) ¹¹⁷ Cd | 273(0.279), 344, 1303 | 5.5 · 10 ⁻³ | 2.5 h | 0.01 | 0.0749 | Yes | 36% | 0% | 33% | 40% | 48% |
| | 1066, 1997(0.262) | 0.6 · 10 ⁻³ | 3.4 h | 0.01 | | Yes | | | | | |
| ⁸⁹ Y (n,n') ^{89m} Y | 909(0.9916) | 1.4 · 10 ⁻³ | 15.7 s | 1.12 | 1 | No | 24% | 43% | 21% | 26% | 0% |
| ⁷⁷ Se (n,n') ^{77m} Se | 162(0.53) | 9.5 · 10 ⁻³ | 17.36 s | 1.87 | 0.763 | No | 0% | 8% | 4% | 5% | 0% |
| ⁷⁹ Br (n,n') ^{79m} Br | 207.2(0.76) | 7.4 · 10 ⁻³ | 4.86 s | 1.82 | 0.5069 | No | 0% | 12% | 6% | 7% | 0% |



Neutron Activation Diagnostic

New Foil Project



Neutron Activation Diagnostic

New Foil Project

2. New germanium detector provides the increasing high energy resolution and high efficiency measurement of the full energy peaks for multi-elements sample.

To use IPPLM's HPGe detector (35% 'effectivnes', coaxial, pre-calibrated)

3. Fast neutron spectrum unfolding method using activation measurements. The method is based on the procedure of minimize following functional:

$$J_x[\varphi(E)] = \int_0^{\infty} [\varphi(E) - \varphi_0(E)]^2 \cdot \sigma_x^2(E) \cdot dE$$

for given reaction type – x, where $\varphi_0(E)$ is a first step approximation of the spectrum, which was obtained from another procedure (e.g. MCNP modelling, TOF)

